The Meteoritical Society

Meteoritics & Planetary Science 42, Nr 7/8, 1055–1075 (2007)
Abstract available online at http://meteoritics.org

Titanium isotopic compositions of well-characterized silicon carbide grains from Orgueil (CI): Implications for *s*-process nucleosynthesis

Gary R. HUSS[1*] and Julie B. SMITH[2]

[1]Hawai‘i Institute of Geophysics and Planetology, University of Hawai‘i at Manoa, 1680 East-West Road, Honolulu, Hawai‘i 96822, USA
[2]Charles Evans & Associates, 810 Kifer Road, Sunnyvale, California 94086, USA
[*]Corresponding author. E-mail: ghuss@higp.hawaii.edu

(Received 16 October 2006; revision accepted 22 April 2007)

Abstract–We have measured the titanium isotopic compositions of 23 silicon carbide grains from the Orgueil (CI) carbonaceous chondrites for which isotopic compositions of silicon, carbon, and nitrogen and aluminum-magnesium systematics had been measured previously. Using the 16 most-precise measurements, we estimate the relative contributions of stellar nucleosynthesis during the asymptotic giant branch (AGB) phase and the initial compositions of the parent stars to the compositions of the grains. To do this, we compare our data to the results of several published stellar models that employ different values for some important parameters. Our analysis confirms that *s*-process synthesis during the AGB phase only slightly modified the titanium compositions in the envelopes of the stars where mainstream silicon carbide grains formed, as it did for silicon. Our analysis suggests that the parent stars of the >1 μm silicon carbide grains that we measured were generally somewhat more massive than the Sun (2–3 $M_\odot$) and had metallicities similar to or slightly higher than solar. Here we differ slightly from results of previous studies, which indicated masses at the lower end of the range 1.5–3 $M_\odot$ and metallicities near solar. We also conclude that models using a standard ^{13}C pocket, which produces a good match for the main component of *s*-process elements in the solar system, overestimate the contribution of the ^{13}C pocket to *s*-process nucleosynthesis of titanium found in silicon carbide grains. Although previous studies have suggested that the solar system has a significantly different titanium isotopic composition than the parent stars of silicon carbide grains, we find no compelling evidence that the Sun falls off of the array defined by those stars. We also conclude that the Sun does lie on the low-metallicity end of the silicon and titanium arrays defined by mainstream silicon carbide grains.

INTRODUCTION

The isotopic compositions of presolar silicon carbide grains provide information about the nucleosynthesis that took place in the parent stars and about the galactic chemical evolution that produced the initial compositions of the parent stars. Most presolar silicon carbide grains (~93%) are known as “mainstream” grains and are believed to come from 1.5 to 3 $M_\odot$ stars in the asymptotic giant branch (AGB) phase, when the stellar envelope becomes carbon-rich (e.g., Lugaro et al. 1999; Amari et al. 2001a). The chemical and isotopic composition of the envelope at the time silicon carbide grains form has been modified by convective episodes, known as the first and third dredge-ups (second dredge-up only occurs in more massive stars), which bring up newly synthesized material from deep in the star (Iben and Renzini 1983; Dearborn 1992; Straniero et al. 1997; Gallino et al. 1998). The isotopic compositions of carbon and nitrogen in the envelope and in grains that form from it provide information on the partial hydrogen burning that took place at the base of the stratified envelope of a star during its main-sequence lifetime and about possible mixing processes at the base of the stratified envelope during the later stages of the star’s life. Magnesium isotopes record the decay of ^{26}Al, which is produced by hydrogen burning (Forestini et al. 1991; Nollett et al. 2003). Silicon isotopes are not strongly affected by stellar nucleosynthesis in low-mass stars, so the silicon compositions of mainstream silicon carbide grains primarily record the initial composition of the star (e.g., Lugaro et al. 1999). In contrast, $^{29,30}Si$-rich compositions of Y and Z grains reflect larger contributions from nucleosynthesis in the parent stars (e.g., Amari et al. 2001a).

Table 1. Characteristics of Orgueil silicon carbide grains chosen for analysis.

Grain	Original size (μm)	Classification, special features	Grain	Original size (μm)	Classification, special features
39	8.8	Mainstream	301	4.5	Unusual composition
49	4.2	Mainstream	302	5.5	Mainstream
52	6.9	Mainstream	307	4.6	Mainstream
58b	6.1	Mainstream, Group IV	317	6.9	Mainstream
70	5.3	Mainstream	320	6.1	Mainstream, Group VI
71	4.9	Mainstream	346	6.0	Mainstream
72	7.8	Mainstream	385	4.2	Mainstream
79	4.0	Mainstream, Group VI	395	4.6	Mainstream
101	4.2	Mainstream, Group IV	416	4.3	Mainstream
106	5.0	Mainstream	432	4.1	Unusual composition
109	5.9	Mainstream	524	4.2	Mainstream
110	4.0	Mainstream, Group IV			

Titanium also appears to record both the initial composition of the star and slow neutron-capture synthesis (*s*-process) in low-mass stars (Hoppe et al. 1994; Gallino et al. 1994; Lugaro et al. 1999; Amari et al. 2001a). Enrichments or deficits of the minor titanium isotopes ^{46,47,49,50}Ti relative to ^{48}Ti provide information on the initial composition of the parent star, while excesses of ^{49,50}Ti relative to the underlying composition provide information about *s*-process nucleosynthesis taking place in the parent star. Model calculations typically show larger *s*-process effects in titanium than in silicon (Gallino et al. 1994; Lugaro et al. 1999; Amari et al. 2001a).

Titanium isotopic compositions have previously been reported from 28 1–10 μm silicon carbide grains from Murchison (Hoppe et al. 1994), 20 grains >1.5 μm from Murchison (Alexander and Nittler 1999), 20 Y grains from Murchison (Amari et al. 2001a), and 30 type A and B grains from Murchison (Amari et al. 2001b). A preliminary report on 75 randomly selected silicon carbide grains from the Murchison KJG fraction (mean diameter 3.02 μm) was presented at the 69th Meteoritical Society Meeting (Gyngard et al. 2006). Most of these were mainstream grains that probably formed in the winds of 1.5 to 3 $M_\odot$ carbon stars. In addition, titanium isotopic compositions have been obtained for 17 X-grains, which are thought to have come from supernovae (Nittler et al. 1996; Hoppe and Besmehn 2002), and from 2 silicon carbide grains that may have come from novae (Nittler and Hoppe 2005). The data for mainstream, Y, Z, and perhaps A and B grains, theoretical studies of titanium nucleosynthesis via the *s*-process (Gallino et al. 1994; Lugaro et al. 1999), and modeling of galactic chemical evolution (Timmes et al. 1995) and stochastic variations in relative contributions from different stellar sources (Lugaro et al. 1999) have provided an overall picture of how titanium isotopes in presolar silicon carbide grains from low- and intermediate-mass stars can be interpreted. However, a number of major questions remain, as will be discussed later in this paper.

In order to extract the maximum information about the parent star of a presolar silicon carbide grain, it is necessary to determine the isotopic compositions of many elements (e.g., Hoppe et al. 1994; Huss et al. 1997). The silicon carbide grains measured in this study came from the Orgueil (CI) carbonaceous chondrite and had previously been measured for silicon, carbon, nitrogen, and magnesium isotopic compositions by Huss et al. (1997). Of the 140 grains measured in that study, 23 were still large enough to measure for titanium. These grains had original diameters of 4.0 to 8.8 μm and included mainstream grains, grains with unusual isotopic composition in other elements, and grains with such similar isotopic compositions that they were interpreted by Huss et al. (1997) to have originated in a the same stellar source. A secondary electron image of grain 320 can be found in Huss et al. (1997), and a preliminary report of the data presented here was given at the 65th Meteoritical Society Meeting (Smith and Huss 2002).

SAMPLES AND EXPERIMENTAL METHODS

The silicon carbide grains measured in this study came from a SiC-spinel separate of Orgueil prepared as part of a study of abundances of presolar diamond, silicon carbide, and graphite in chondrites (Huss and Lewis 1995). The grains were identified and characterized in a study of 140 Orgueil silicon carbide grains carried out by Huss et al. (1997), who measured the isotope compositions of silicon, carbon, nitrogen, and magnesium in the grains. The largest surviving grains from the Huss et al. (1997) study were measured in this study. All were larger than 4 μm. A summary of the characteristics of the grains is presented in Table 1.

The grains were measured with the Cameca ims 6f ion microprobe at Arizona State University. An O^- primary beam defocused to ~25 μm was used. The secondary-ion mass spectrometer was operated with an imaged field of ~75 μm (to increase transmission) and a mass-resolving power of ~4550 (M/ΔM, 10% definition). The masses measured were ^{28}Si, ^{40}Ca, ^{42}Ca, ^{44}Ca, ^{46}Ti, ^{47}Ti, ^{48}Ti, ^{49}Ti,

^{50}Ti, and ^{52}Cr. Corrections were made for interferences from ^{46}Ca on ^{46}Ti, ^{48}Ca on ^{48}Ti, and ^{50}Cr on ^{50}Ti based on isotopic ratios of terrestrial calcium and chromium. Separating the interferences from ^{46}Ca and ^{50}Cr requires a mass resolving power of ~40,000, so the peaks overlap almost completely, and the contribution to masses 46 and 50 from calcium and chromium calculated from measurements of ^{40}Ca and ^{50}Cr can be subtracted directly. However, ^{48}Ca can be resolved from ^{48}Ti with a mass resolving power of ~10,000, so the peaks are partially resolved at a mass resolving power of ~4550. Therefore, the correction on ^{48}Ti was made as a "tail correction." The shape of the ^{48}Ti peak was determined and the height of the "tail" at the distance from the center on the low side of the ^{48}Ti peak corresponding to the difference in peak positions of ^{48}Ca and ^{48}Ti was measured. This gives the height of the tail of the ^{48}Ca peak at the center of the ^{48}Ti peak. The correction was then made by multiplying the measured ^{40}Ca intensity by the ^{48}Ca/^{40}Ca ratio and by the fractional height of the "tail," and then subtracting the result from the ^{48}Ti peak. Because the calcium contents were lower than the titanium contents, and because most of the calcium is ^{40}Ca, the corrections for calcium interferences were always small, <<1%. The correction for ^{50}Cr on ^{50}Ti was larger, ranging from 0.2% in grain 79 up to ~90% for grain 106, but were typically <10%. The largest correction on ^{50}Ti for grains discussed in detail in this paper was ~35% for grain 58b.

No correction was made for instrumental mass fractionation, both because it is small compared to our uncertainties and the observed effects, and because we did not have a suitable matrix-matched standard to determine the fractionation. A correction was made for electron multiplier background of 0.007 cps. Reported uncertainties are the 2-sigma counting uncertainties for the ratios combined with statistical uncertainties for the background correction and any interference corrections. A non-statistical uncertainty of 20% of the interference correction was combined with the statistical uncertainty for ^{50}Ti/^{48}Ti. This reflects the variability of the interfering signals over the course of the run, which is not perfectly corrected for by subtracting an average value for the interference, and uncertainties in the isotopic compositions of the interfering elements. It thus has both systematic and random components.

RESULTS

The ^{48}Ti/^{28}Si ratio and the titanium isotopic ratios and delta values determined in this study are presented in Table 2. Also shown are the delta ^{29,30}Si values for the grains from Huss et al. (1997). Delta values are the deviation of the measured composition from the standard ratios (shown at the top of the table) in parts per thousand (see footnote). The discussion will concentrate on the 16 grains at the top of the table, the grains with the smallest errors.

Titanium Abundances

Although we did not standardize our measurements to determine the titanium abundance in each grain, we can roughly estimate the abundances from the measured ^{48}Ti/^{28}Si ratios and the relative ionization efficiency of the two elements. The useful yield (the inverse of the relative sensitivity factor [RSF]) of titanium in silicon is ~10 times higher than silicon under oxygen bombardment (e.g., Wilson and Novak 1991). From this we estimate the titanium content of the silicon carbide grains to range from ~40 ppm to 0.3%. In many of the grains, the titanium is probably in subgrains of titanium carbide (e.g., Bernatowicz et al. 1996). The variations in the ^{48}Ti/^{28}Si ratio over the course of the measurement for many grains clearly show the presence of these subgrains (Fig. 1). For grains with high titanium content, ^{48}Ti/^{28}Si ratios remained nearly constant during a run, probably reflecting a large number of small titanium carbide grains. But a nearly constant ^{48}Ti/^{28}Si ratio could also indicate that titanium is replacing silicon in the silicon carbide structure. We do not see any evidence of isotopic differences among the subgrains, but we would only be able to detect very large differences, which are not expected from our understanding of nucleosynthesis in low-mass stars.

Isotopic Data

The titanium isotopic data for the 16 grains with the smallest errors are shown in Figs. 2 and 3. Grains in Fig. 2 are arranged in order of increasing δ^{29}Si from top to bottom. Note that the $\delta^{46,47,49,50}$Ti values only generally correlate with the δ^{29}Si values. All but one of the grains shows excesses in all of the isotopes relative to the terrestrial standard. The exception, grain 301, has a significant deficit of ^{50}Ti, while the other isotopic ratios are close to the terrestrial values. The interference correction for ^{50}Ti is not responsible for the negative δ^{50}Ti value. Figure 3 shows grains from Groups IV and VI that were interpreted by Huss et al. (1997) to represent two individual stellar sources. These grains have essentially identical isotopic compositions of carbon, silicon, nitrogen, and, where data are available, inferred ^{26}Al/^{27}Al ratio. The group IV grains are generally similar to each other, but there are significant differences. For grain 58B, there was a very large correction to the ^{50}Ti abundance, but it is unlikely that the correction caused this grain to differ from the others. The grains also differ in abundances of the low-mass isotopes. In contrast, the Group VI grains have essentially identical titanium compositions, supporting the idea that they might come from the same stellar source.

Figures 4 and 5 plot $\delta^{46,47,49,50}$Ti for the 16 grains with the smallest errors against ^{29}Si and ^{30}Si, respectively. Also shown are the previously published data for mainstream grains. For the most part, our data fall within the range of previous data.

Table 2. Titanium data and silicon compositions of well-characterized Orgueil silicon carbide grains.

Grain	$^{48}Ti/^{28}Si$	$^{46}Ti/^{48}Ti$	$^{47}Ti/^{48}Ti$	$^{49}Ti/^{48}Ti$	$^{50}Ti/^{48}Ti$	$\delta^{29}Si$	$\delta^{30}Si$	$\delta^{46}Ti$	$\delta^{47}Ti$	$\delta^{49}Ti$	$\delta^{50}Ti$
Standard ratios[a]		0.108548	0.099315	0.074463	0.072418	0.0506331	0.033464				
39	0.008562 (58)	0.1170 (16)	0.1015 (14)	0.0777 (12)	0.0824 (14)	65.4 (3.5)	68.4 (3.5)	78 (14)	22 (14)	43 (17)	138 (20)
49	0.00882 (18)	0.1238 (54)	0.1043 (50)	0.0830 (46)	0.0863 (47)	128.3 (5.2)	104.9 (6.3)	141 (50)	51 (50)	115 (62)	192 (65)
52	0.02197 (17)	0.1206 (18)	0.1040 (16)	0.0809 (14)	0.0838 (16)	68.7 (4.3)	65.4 (4.6)	111 (16)	47 (16)	86 (19)	157 (23)
58b	0.000587 (5)	0.1163 (19)	0.1007 (18)	0.0784 (16)	0.0764 (51)	47.7 (4.1)	51.5 (3.7)	71 (18)	14 (18)	52 (21)	55 (71)
70	0.00722 (12)	0.1246 (33)	0.1054 (30)	0.0810 (26)	0.0826 (28)	81.0 (7.2)	78.2 (6.9)	148 (31)	61 (31)	88 (35)	140 (39)
72	0.01014 (11)	0.1164 (25)	0.1030 (24)	0.0801 (21)	0.0804 (21)	50.8 (3.9)	51.5 (4.0)	73 (23)	37 (24)	75 (28)	110 (29)
79	0.03899 (39)	0.1347 (24)	0.1107 (21)	0.0857 (18)	0.0998 (20)	168.3 (6.1)	141.9 (6.3)	241 (22)	115 (21)	151 (24)	378 (27)
101	0.01990 (22)	0.1222 (27)	0.1044 (24)	0.0802 (21)	0.0906 (23)	46.1 (3.0)	55.6 (3.7)	125 (25)	52 (25)	77 (28)	251 (31)
110	0.02591 (59)	0.1160 (56)	0.1007 (52)	0.0807 (46)	0.0879 (48)	48.5 (6.8)	59.5 (7.5)	69 (51)	14 (52)	84 (62)	214 (67)
301	0.01805 (20)	0.1111 (26)	0.0986 (24)	0.0748 (21)	0.0663 (23)	−27.7 (2.8)	−16.2 (4.5)	23 (24)	−7 (24)	5 (28)	−85 (31)
317	0.01663 (11)	0.1131 (14)	0.1008 (13)	0.0792 (12)	0.0804 (12)	−9.4 (2.3)	35.4 (3.4)	42 (13)	15 (14)	64 (16)	110 (16)
320	0.007581 (81)	0.1338 (27)	0.1081 (24)	0.0866 (21)	0.0997 (23)	166.9 (4.0)	136.6 (4.6)	233 (25)	88 (24)	163 (29)	377 (32)
346	0.03024 (16)	0.1141 (11)	0.1011 (11)	0.0778 (9)	0.0778 (9)	47.1 (2.8)	55.9 (3.9)	51 (11)	18 (11)	45 (12)	74 (13)
416	0.006647 (63)	0.1168 (22)	0.1024 (21)	0.0797 (18)	0.0799 (19)	52.6 (3.5)	57.5 (4.2)	76 (21)	31 (21)	71 (24)	103 (26)
432	0.001458 (71)	0.1138 (57)	0.1023 (53)	0.0766 (47)	0.0770 (47)	68.6 (3.9)	71.9 (3.9)	49 (52)	30 (54)	29 (63)	63 (65)
524	0.00816 (39)	0.1266 (62)	0.1059 (57)	0.0797 (50)	0.0799 (50)	66.3 (2.9)	53.6 (5.3)	167 (57)	66 (57)	71 (67)	103 (69)
71	0.000397 (35)	0.119 (27)	0.108 (26)	0.058 (22)	0.075 (29)	86.6 (8.5)	83.3 (12.3)	92 (245)	85 (259)	−222 (294)	36 (405)
106	0.0216 (18)	0.085 (23)	0.101 (24)	0.082 (23)	0.049 (40)	39.5 (3.6)	32.9 (4.1)	−220 (211)	20 (242)	100 (306)	−321 (549)
109	0.000843 (58)	0.111 (16)	0.090 (15)	0.059 (12)	0.072 (19)	27.0 (24.1)	38.7 (24.9)	21 (150)	−90 (147)	−201 (161)	−10 (264)
302	0.000400 (30)	0.123 (24)	0.112 (23)	0.094 (22)	0.074 (20)	95.0 (2.8)	87.4 (3.9)	138 (221)	127 (227)	266 (294)	23 (275)
307	0.00220 (17)	0.110 (23)	0.103 (23)	0.077 (22)	0.084 (22)	53.2 (4.7)	60.1 (5.2)	17 (212)	37 (229)	32 (291)	153 (310)
385	0.00516 (21)	0.113 (10)	0.0962 (98)	0.0812 (93)	0.088 (10)	49.0 (3.4)	59.8 (4.4)	37 (95)	−31 (99)	90 (125)	213 (139)
395	0.000672 (31)	0.109 (17)	0.105 (16)	0.075 (15)	0.067 (16)	107.0 (3.1)	93.9 (3.3)	7 (153)	59 (166)	1 (208)	−80 (224)

[a]Standard ratios for titanium from Niederer et al. (1985), for $^{29}Si/^{28}Si$ from Barnes et al. (1975), and for $^{30}Si/^{28}Si$ from Stone et al. (1991).

Delta values are found from: $\delta^{xx}Ti = \{[(^{xx}Ti/^{48}Ti)_{measured}/(^{xx}Ti/^{48}Ti)_{standard}] - 1\} \times 1000$ and similarly for silicon. 2σ uncertainties are shown in parentheses.

Both sets of data show a correlation between the silicon isotopic composition and the titanium isotopic composition.

DISCUSSION

Relative Contributions of Initial Compositions of Parent Stars and Stellar Nucleosynthesis

General Considerations

The distributions of silicon and titanium isotopes in mainstream silicon carbide grains have been interpreted in terms of the initial compositions of the parent stars overprinted by *s*-process nucleosynthesis in the parent stars (e.g., Hoppe et al. 1994; Gallino et al. 1994; Huss et al. 1997; Alexander and Nittler 1999; Lugaro et al. 1999). Detailed modeling of nucleosynthesis in low-mass AGB stars suggests that the initial compositions of the parent stars dominate the silicon-isotope array for mainstream grains (e.g., Gallino et al. 1994; Lugaro et al. 1999; Zinner et al. 2006). Titanium isotopes are less well understood, but a somewhat larger role for *s*-process synthesis has been inferred (e.g., Amari et al. 2001a).

Unlike the CNO isotopes, which are strongly affected by nucleosynthesis in low-mass stars, silicon and titanium isotopes are only weakly affected. Nuclear processing of silicon and titanium takes place late in the star's life, during the AGB phase, when hydrogen and helium burn alternately in shells surrounding the carbon-oxygen core. Detailed discussions of the structure and evolution of low-mass stars are given in Iben and Renzini (1983), Straniero et al. (1997, 2006), and Gallino et al. (1998). When the helium shell ignites, the resulting thermal instability drives convective mixing in the whole helium intershell. About 1000 years after the quenching of this convective instability, the border of the overlying convective envelope penetrates into the upper region of the helium intershell, bringing to the surface fresh nucleosynthetic products (known as third-dredge-up events). Silicon and titanium are transmuted via slow neutron capture (*s*-process). Two neutron sources are available. The reaction, $^{13}C(\alpha,n)^{16}O$, produces neutrons in the top layers of the radiative intershell region between the hydrogen and helium shells during the quiescent period when the hydrogen shell is active. During third dredge-up mixing events, hydrogen is mixed into the ^{12}C-rich intershell region. When hydrogen burning resumes, ^{12}C burns by proton capture to ^{13}C (and ^{14}N). Later on, ^{13}C suffers alpha capture and neutrons are released. This "^{13}C pocket" generates neutrons at relatively low temperature. A higher-temperature source of neutrons is the reaction, $^{22}Ne(\alpha,n)^{25}Mg$, which is marginally activated during thermal pulses when the temperature at the base of the helium shell is sufficiently high. Changes in silicon isotopes are dominated by the high-temperature ^{22}Ne source. For titanium, ^{50}Ti and to a lesser extent ^{49}Ti are produced by neutron-capture at low temperatures in the ^{13}C pocket, while all isotopes are affected, but to a lesser extent, by the high-temperature ^{22}Ne source. Thus, *s*-process effects on silicon and titanium are somewhat decoupled.

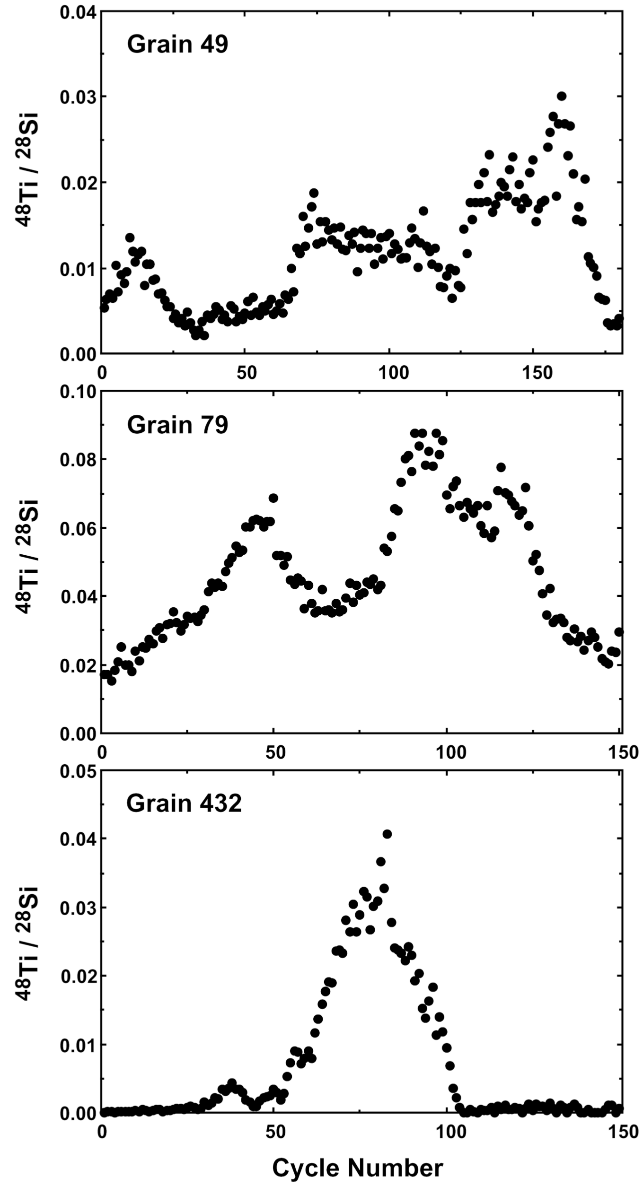

Fig. 1. $^{48}Ti/^{28}Si$ ratios are plotted as a function of measurement cycle for three silicon carbide grains. The large increases in the ratio reflect the presence of subgrains of titanium carbide within the silicon carbide grains.

In principle, one should be able to separate the contributions of initial composition, which represents a mixture of nucleosynthesis products from all types of stars, and *s*-process synthesis in the low-mass parent stars of the silicon carbide grains. Lugaro et al. (1999), in a detailed study of silicon isotopes in AGB stars and in silicon carbide grains, concluded that the *s*-process contribution was small, consistent with 1.5 to 3.0 $M_{\odot}$ parent stars for the majority of

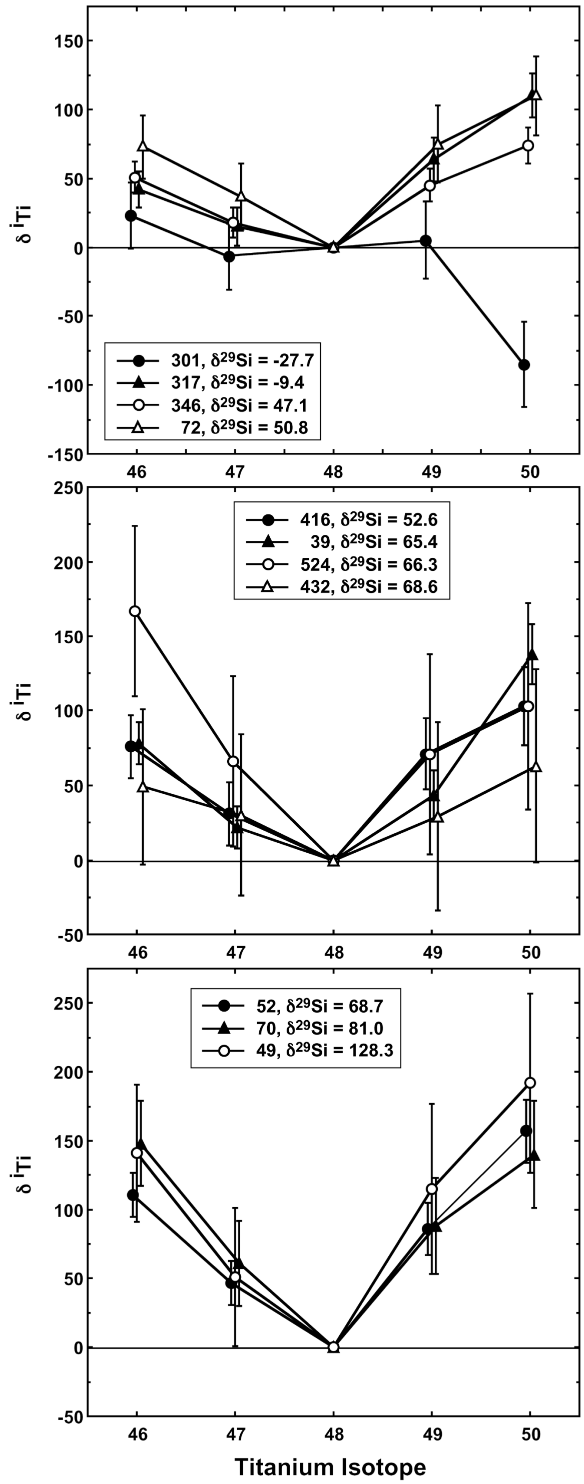

Fig. 2. Titanium isotopic ratios, presented as delta values relative to terrestrial titanium, are shown for 11 of the 16 silicon carbide grains with the smallest measurement errors. All but one of the grains show excesses of minor titanium isotopes compared to the solar composition. There is general increase in $\delta^{46,47,49,50}$Ti values with increasing δ^{29}Si (given in the legend for each grain), but not a tight correlation, reflecting the influences of both initial composition and *s*-process within the star.

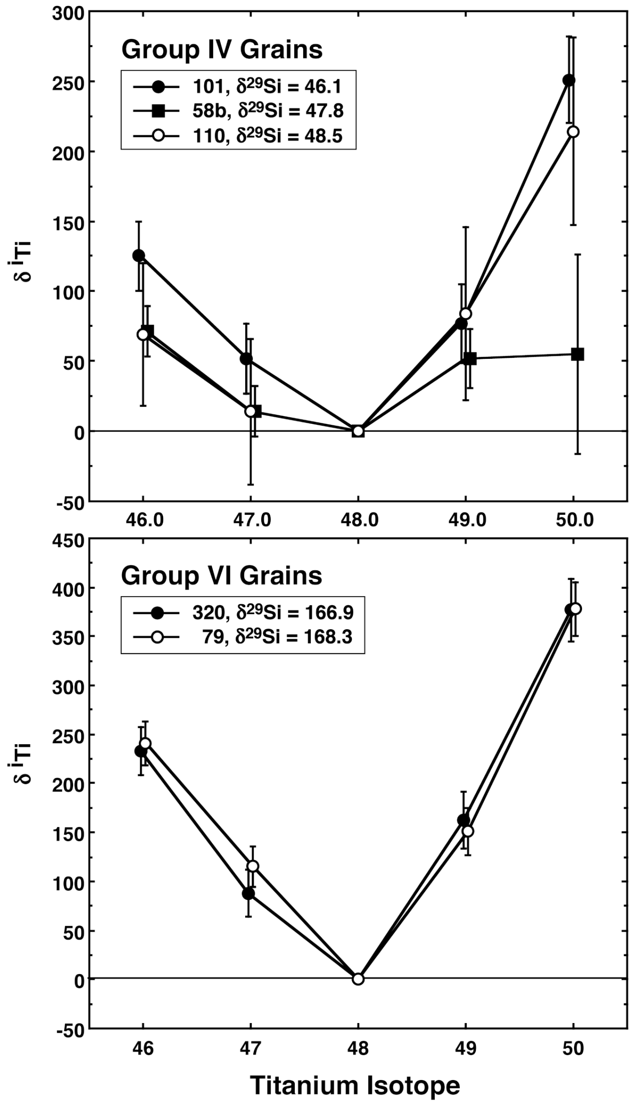

Fig. 3. Titanium isotopic ratios, presented as delta values relative to terrestrial titanium, are shown for five silicon carbide grains suggested by Huss et al. (1997) to belong to two groups of grains that may have originated from individual stellar sources. The grains identified by Huss et al. (1997) as belonging to group IV do not have the same titanium isotopic compositions. However, the two grains that comprise group VI do have the same titanium compositions, supporting the idea that they formed in the same stellar source.

grains. Amari et al. (2001a) took this work a step further to calculate the initial compositions of the Y grains, which have larger AGB contributions. These authors derived a linear array of initial compositions that plots as a line of slope 1.31 and an intercept value of δ^{29}Si = −3.2‰ at δ^{30}Si = 0 on a plot of δ^{29}Si versus δ^{30}Si. They then projected the measured compositions to this array of initial compositions along slope 0.5-lines (predicted by *s*-process models) and thereby were able to estimate the initial compositions of the parent stars (Fig. 7 of Amari et al. 2001a). Zinner et al. (2006) did a similar analysis of the data from a large number of silicon

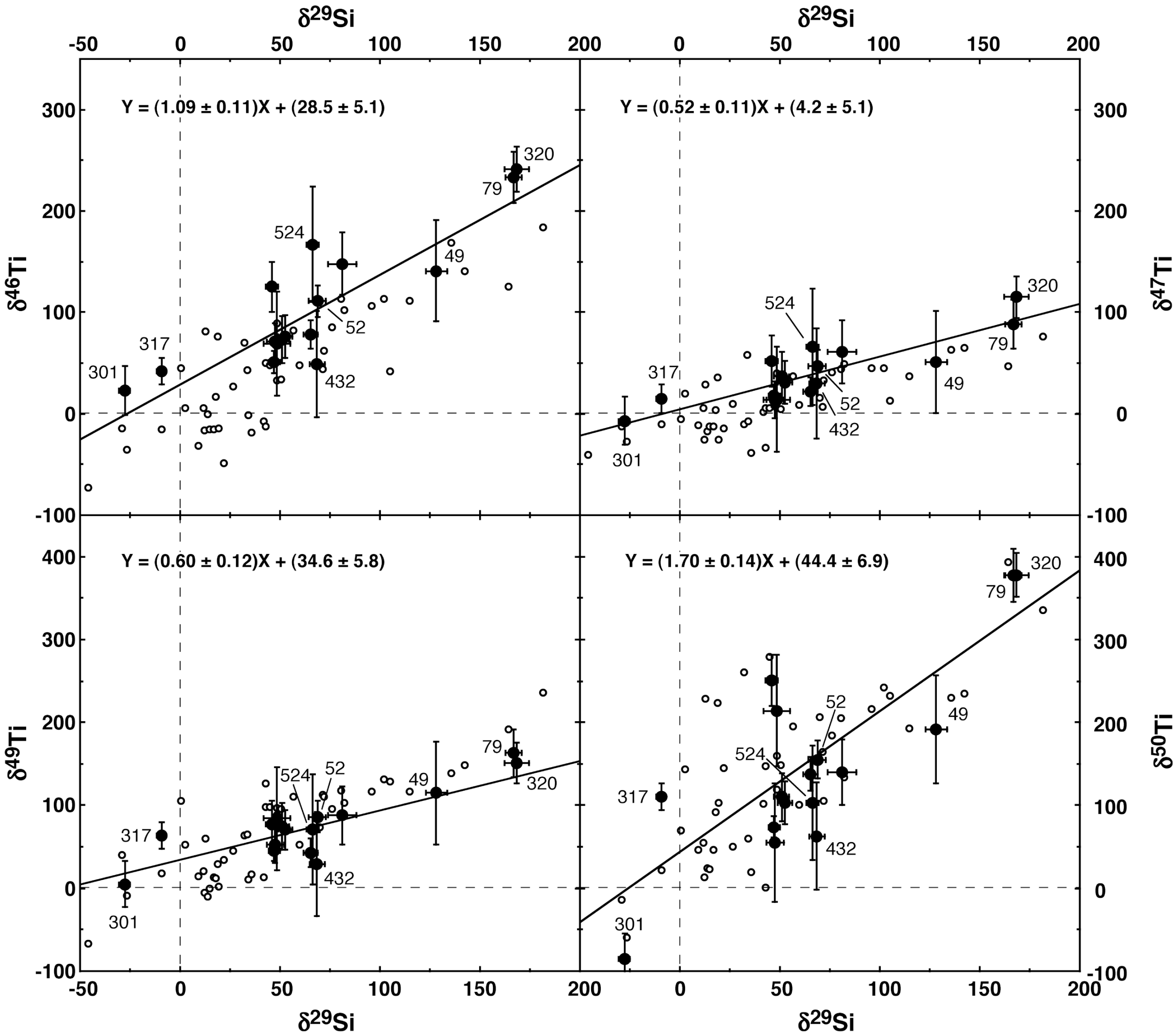

Fig. 4. Titanium isotopic ratios, presented as delta values relative to terrestrial titanium, are plotted against δ^{29}Si. There is a reasonably strong correlation between the titanium ratios and δ^{29}Si. The solid lines through the data points are error-weighted, least-squares regressions through the data. The correlation lines pass close to the solar-system composition (=terrestrial composition), indicated by the light dashed lines. Grains discussed explicitly in the text are identified. Open symbols show literature data for mainstream grains from Hoppe et al. (1994) and Alexander and Nittler 1999. (Two extreme literature values fall off the δ^{50}Ti plot, one at very high δ^{50}Ti and moderate δ^{29}Si, and one at low δ^{50}Ti and low δ^{29}Si.)

carbide grains using different models for the silicon isotopes and found a similar result. These studies confirm that most of the range of silicon isotope compositions for mainstream grains is due to the initial compositions of the parent stars.

Amari et al. (2001a) extended this approach to the titanium isotopes. Using the model data for 1.5 and 3.0 $M_\odot$ stars, and a range of neutron exposures in the ^{13}C pocket, they attempted to estimate the initial titanium compositions of the source stars for the silicon carbide grains based on the regression lines through the compositions for the grains. As expected from the neutron-capture cross sections for the titanium isotopes, the inferred arrays of initial compositions for δ^{46}Ti and δ^{47}Ti did not shift much from the observed data arrays. However, the inferred arrays of initial compositions for δ^{49}Ti and δ^{50}Ti were displaced significantly from the array of grain compositions and from the solar composition. Amari et al. (2001a) tentatively concluded that the solar system composition is anomalous in that it does not lie on the arrays of initial compositions inferred for the parent stars of the silicon carbide grains. However, Alexander and Nittler (1999), by doing χ^2 fitting to the grain data, concluded that the solar system does not have an especially anomalous titanium isotope composition compared to silicon carbide parent stars.

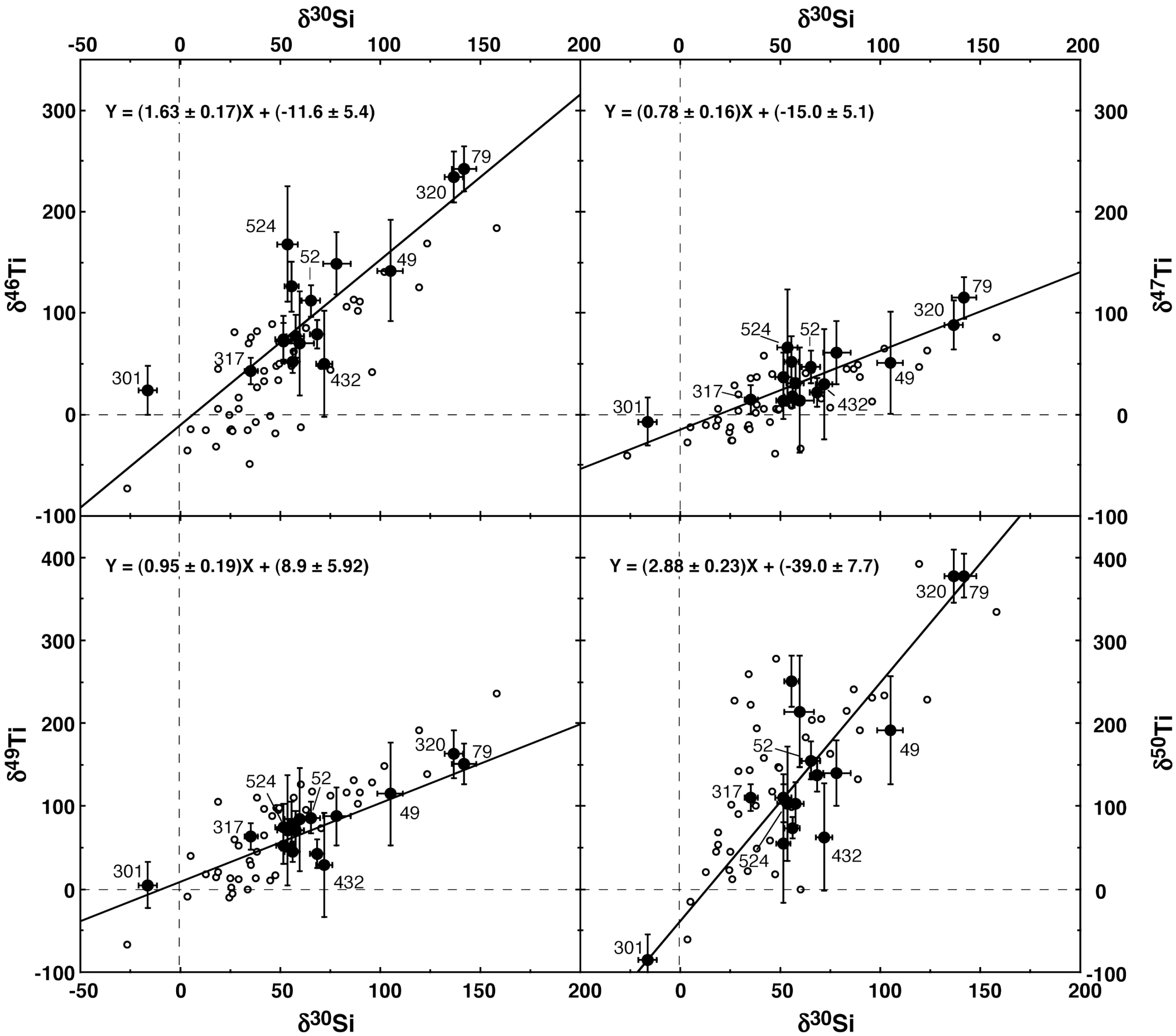

Fig. 5. Titanium isotopic ratios, presented as delta values relative to terrestrial titanium are plotted against δ^{30}Si. There is a reasonably strong correlation between the titanium ratios and δ^{30}Si, but the correlation is not as strong as with δ^{29}Si, as shown by the uncertainties in the fits to the data. The error-weighted, least-squares regressions through the data pass close to the solar-system composition (=terrestrial composition), indicated by the light dashed lines. Grains discussed explicitly in the text are identified. Open symbols show literature data for mainstream grains from Hoppe et al. (1994) and Alexander and Nittler 1999. (Two extreme literature values fall off the δ^{50}Ti plot, one at very high δ^{50}Ti and moderate δ^{30}Si and one at low δ^{50}Ti and low δ^{30}Si.)

In this paper, we again attempt to separate the contributions of initial composition and *s*-process nucleosynthesis to the measured compositions of the silicon carbide grains. To do so, we evaluate the roles of several different parameters that affect the silicon and titanium compositions predicted by the models. Parameters in stellar models that affect the *s*-process yields and compositions include: 1) neutron-capture cross sections, 2) stellar metallicity, 3) stellar mass, 4) the strength of the ^{13}C neutron source, and 5) the mass-loss rate during the AGB phase (Gallino et al. 1998; Lugaro et al. 1999; Zinner et al. 2006). We will address the effects and uncertainties of each parameter and then attempt to establish the most promising ranges to explain the grain data. For this discussion, we will use models for 1.5, 3.0, and 5.0 $M_{\odot}$ stars published by Lugaro et al. (1999) and Amari et al. (2001a). We couple these models with the new results for silicon isotopes published by Zinner et al. (2006). Although we will only discuss our data set, the conclusions should be general because our data set has the same characteristics as other data sets (Figs. 4 and 5).

Neutron-Capture Cross Sections: Neutron-capture cross sections are a key input to *s*-process calculations. Neutron-capture cross sections for silicon and titanium isotopes used in the models we discuss here still have relatively large uncertainties (e.g., Lugaro et al. 1999). New measurements of the cross sections for silicon isotopes made by Guber et al. (2003) are significantly different from those used previously (e.g., Bao et al. 2000, based on experimental data by Boldeman et al. 1975). The new measurements of silicon cross sections were motivated by the requirements of detailed stellar models of *s*-process nucleosynthesis and are far more accurate than the previous values. The new cross sections lead to much larger isotopic shifts in ^{30}Si in model calculations, and the slope of the *s*-process evolution on a silicon three-isotope plot (Fig. 6) decreases substantially (e.g., from 0.82 to 0.17 in one model and from 0.42 to 0.08 in another; Zinner et al. 2006). The change is due to smaller cross sections for ^{28}Si(n,γ)^{29}Si, which results in lower ^{29}Si/^{28}Si ratios, and a smaller cross section for ^{30}Si(n,γ)^{31}Si, which slows the destruction of ^{30}Si and results in higher ^{30}Si/^{29}Si ratios. The effects of the new cross sections are discussed by Zinner et al. (2006). Neutron-capture cross sections for titanium are still quite uncertain, but the general features of *s*-process nucleosynthesis should be adequately modeled (e.g., Lugaro et al. 1999). We discuss potential effects of errors in the cross sections below.

Stellar Metallicity: The metallicity of a star affects the *s*-process yields. The number of neutrons from the ^{13}C neutron source does not depend strongly on the metallicity of the star because the ^{13}C is produced by proton capture on ^{12}C produced from partial helium burning in the convective shell (Gallino et al. 1998; Lugaro et al. 1999). The initial abundances of ^{12}C and ^{13}C in the star are not important. All other things being equal, the metallicity changes the number of seed nuclei available to react with the approximately constant number of neutrons. So for low-metallicity stars, there are more neutrons per seed nucleus than in high-metallicity stars (e.g., Gallino et al. 1998), and to first order, one should expect larger *s*-process shifts in titanium isotopes for low-metallicity stars.

Metallicity also effects the silicon isotopes, but for a different reason. The silicon isotopes are primarily affected by the ^{22}Ne source, which is marginally activated at the base of the helium shell during later thermal pulses of the AGB phase (Lugaro et al. 1999). Temperatures are higher in low-metallicity stars, so the ^{22}Ne source is more efficient, giving rise to larger isotopic effects in silicon isotopes (Gallino et al. 1998; Lugaro et al. 1999).

Finally, one must remember that metallicity has a strong effect on the initial isotopic compositions of both silicon and titanium. As already discussed, the arrays in Figs. 4–6 primarily reflect differences in the initial compositions of the stars due to the effects of galactic chemical evolution.

Stellar Mass: As the mass of the star increases, temperatures and rates of neutron capture reactions increase. Although all

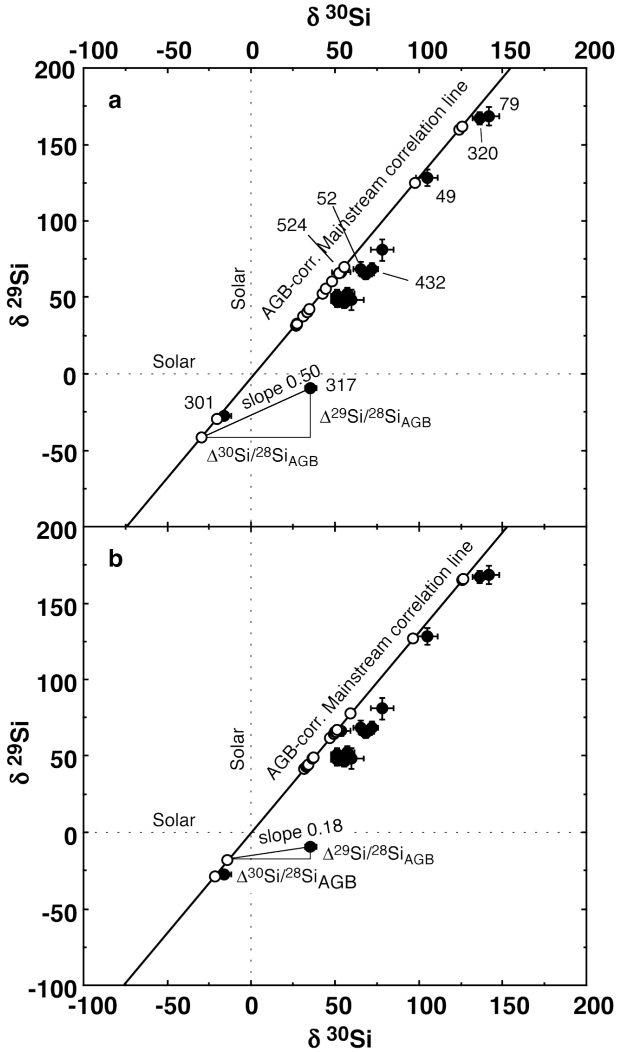

Fig. 6. Measured δ^{29}Si and δ^{30}Si values the silicon carbide grains are shown as solid symbols on these silicon three-isotope plots. Theoretical arrays of initial compositions for the parent stars (solid lines with slope 1.31, see text for explanation) are also shown. Dashed lines show the solar composition. The open symbols show the compositions of the grains after correction for the supposed AGB contribution from the parent star based on stellar models. In panel a, the model calculation uses the neutron capture cross sections of Bao et al. (2000), which result in shifts along slope ~0.5 lines. An example of the shift due to AGB synthesis is shown. In panel b, the model calculation uses neutron-capture cross sections from Guber et al. (2003), which result in shifts along slope ~0.18 lines. Note that shifts are smaller when the Guber et al. (2003) cross sections are used.

reaction rates depend strongly on temperature, their dependences differ sufficiently to change the composition of the *s*-process products. The ^{22}Ne neutron source becomes more important as stellar mass increases because the temperature of the helium shell increases with stellar mass (e.g., Straniero et al. 2006). Third-Dredge-Up becomes more effective with increasing stellar mass (Lugaro et al. 1999;

Straniero et al. 1997), and mass-loss rate increases (e.g., Iben and Renzini 1983). The net effect of these dependences is that isotopic shifts increase with increasing stellar mass (Lugaro et al. 1999; Zinner et al. 2006).

Strength of the ^{13}C Neutron Source: As discussed above, the *s*-process in low-mass stars results from two different neutron sources, which operate in different locations and are initiated at different temperatures. Because the two sources affect silicon and titanium differently, *s*-process effects on silicon and titanium are somewhat decoupled. A significant problem in stellar nucleosynthesis models is that the ^{13}C pocket does not arise in a self-consistent way. It must be introduced by a parameterization (Gallino et al. 1998; Lugaro et al 1999; Straniero et al. 2006). Thus, in addition to the decoupling of the *s*-process effects in silicon and titanium in nature, there is an even greater potential decoupling in the models.

Mass-Loss Rate: Mass-loss rate can significantly affect the yield of *s*-process isotopes. As the mass of the envelope decreases through massive stellar winds, the temperature at the base of the envelope, where the hydrogen burning shell and helium shell are located, decreases. If enough mass is lost, nuclear burning ceases entirely. On the other hand, as the mass of the envelope decreases, the dredged up material is less diluted. The effects of mass loss on silicon-isotope evolution during the AGB in low-mass stars are discussed by Zinner et al. (2006).

Deconvolving the Orgueil Silicon Carbide Data

Silicon Isotopes: In order to estimate the *s*-process contribution in the silicon compositions of the silicon carbide grains, we have followed the lead of Amari et al. (2001a) and assumed an array of initial compositions with a slope 1.31 on a silicon 3-isotope plot. For simplicity, we assume no spread around the array of initial compositions, although clearly there must have been a spread (Alexander and Nittler 1999; Lugaro et al. 1999). Based on *s*-process calculations that used the neutron capture cross sections of Bao et al. (2000), Amari et al. (2001a) inferred that their initial array should intersect the solar δ^{30}Si at δ^{29}Si = −3.2‰. Subsequent work by Zinner et al. (2006), showed that the newer cross sections from Guber et al. (2003) produce larger shifts in δ^{30}Si than the Bao et al. (2000) cross sections. Based on this work, we have defined a second array with the same slope that is shifted to the left so that it passes through the solar composition. This has the effect of increasing the inferred shift from δ^{30}Si by ~2.4‰. This shift is not the result of detailed calculations, but is of the correct sign and approximately the correct magnitude based on the output from published stellar models (e.g., Zinner et al. 2006).

Using these "AGB-corrected galactic arrays," we have removed an estimated *s*-process contribution from the silicon isotopic compositions of each of the Orgueil silicon carbide grains. Figure 6a shows the results using an *s*-process component with a slope of 0.5, based on models using the Bao et al. (2000) cross sections, and the AGB-corrected array defined by Amari et al. (2001a). Figure 6b shows the results of removing an *s*-process component with a slope of 0.18, based on models using Guber et al. (2003) cross sections, and the AGB-corrected array that passes through the solar composition. The slopes for the *s*-process components are average values based on the range of slopes generated by individual models (Amari et al. 2001a; Zinner et al. 2006). In spite of these simplifications, the calculations illustrate some important features. First, the *s*-process contribution necessary to bring the measured silicon compositions to the AGB-corrected array is smaller using the newer cross sections (Fig. 6). Second, the newer cross sections shift the distribution of inferred initial ^{29}Si values for the parent stars to higher ^{29}Si values (Fig. 6).

Titanium Isotopes: Our treatment of the titanium isotopes differs from that presented by Amari et al. (2001a). Instead of subtracting the average predicted AGB contribution from the titanium isotopic compositions of the grains to infer the original ratios of the parent stars, we subtract a contribution from each grain based on the *s*-process shift that we calculated for the silicon isotopes. We will investigate the role of the five factors we described above to find the most reasonable set of parameters to translate the *s*-process shift from silicon to titanium.

Figure 7 compares the measured titanium isotopic compositions of the grains with two sets of calculated compositions. In the first set, the size of the *s*-process component for titanium was inferred from the corrections necessary to move the silicon isotopic compositions to the AGB-corrected mainstream correlation line on Fig. 6a. The titanium composition was shifted based on a stellar model for a 1.5 $M_{\odot}$ star, solar metallicity (0.02), a "standard" value for the ^{13}C pocket, and a Reimers (1975) mass-loss parameter of $\eta = 0.3$ (Lugaro et al. 1999). The second set uses an *s*-process component derived based on the slope of 0.18 (Fig. 6b) to determine the size of the titanium *s*-process component. The titanium ratios were shifted based on the Lugaro et al. (1999) model coupled to the results of the Zinner et al. (2006) models for the same mass, metallicity, ^{13}C pocket, and mass-loss rate using the new silicon cross sections of Guber et al. (2003). Note that the Zinner et al. (2006) model using the Bao et al. (2000) cross sections gave very similar silicon results to the Lugaro et al. (1999) model. To couple the new *s*-process silicon composition to the Lugaro et al. (1999) model, we have adjusted silicon delta values by average factors estimated from the comparisons of models run with Bao et al. (2000) and Guber et al. (2003) cross sections by Zinner et al. (2006). The new cross sections increase the ^{30}Si values by a factor of ~1.75 and decrease the δ^{29}Si values by a factor of

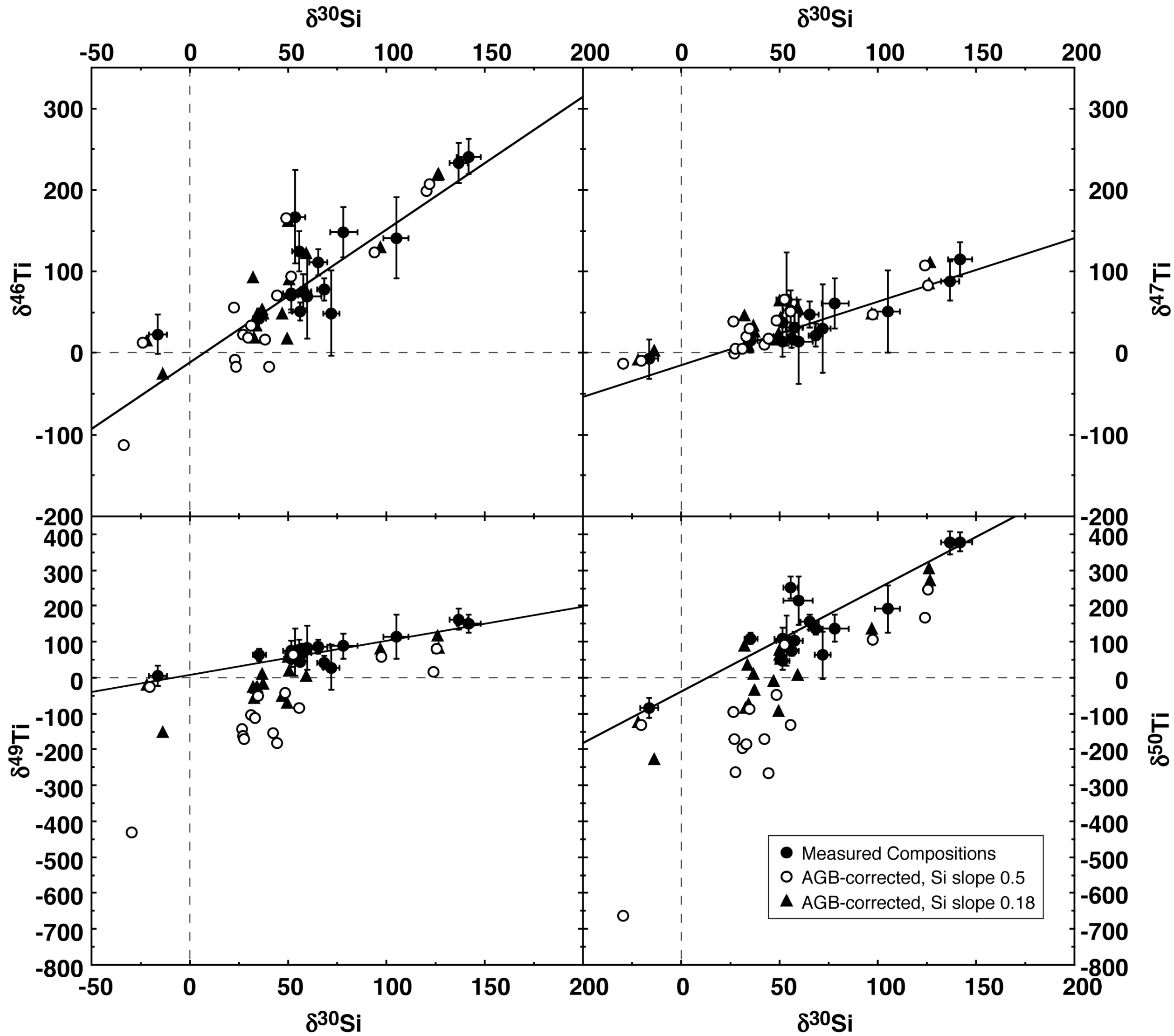

Fig. 7. The measured delta values for titanium, plotted against $\delta^{30}Si$, are compared with AGB-corrected initial compositions for the parent stars calculated based on stellar models using two different sets of neutron-capture cross sections for silicon isotopes (see text). The isotopic shifts are smaller for the calculation that uses results based on the new Guber et al. (2003) cross sections (slope 0.18). Note that the older cross sections generate compositions for the parent stars of some silicon carbide grains that are implausible, requiring extreme contributions to $\delta^{49}Ti$ and $\delta^{50}Ti$ from *s*-process in the parent stars.

~0.3. These factors are not sensitive to other model parameters (Zinner et al. 2006). The calculations were based on the final compositions of the envelope generated in these models. In all of our calculations, an uncertainty results from using the final compositions because the relative abundances of the silicon and titanium isotopes do not evolve linearly (see Lugaro et al. 1999). But these uncertainties that result from coupling different models and from using the final calculated compositions should not obscure the big picture.

Figure 7 plots the delta values for the titanium isotope obtained from our two sets of calculations versus the two sets of $\delta^{30}Si$ values obtained in Figs. 6a and 6b. Several important features are shown. First, the isotopic shifts are relatively small for $\delta^{46}Ti$ and $\delta^{47}Ti$ and tend to be nearly parallel to the original regression lines through the data. The shifts are significantly larger for $\delta^{49}Ti$ and $\delta^{50}Ti$, and move the grains off of the original correlation lines. These observations are consistent with the previous analysis by Amari et al. (2001a). But it is important to note that for a few individual grains, the shifts calculated using the older silicon cross sections are implausibly large. For the grain plotting in the lower left of the bottom panels (grain 317), the calculation using the older cross sections requires that more than 75% of the ^{50}Ti in this grain was produced by the *s*-process in the parent star. The titanium composition of this grain is not unusual compared to the other grains (Fig. 2), so this large shift seems unwarranted.

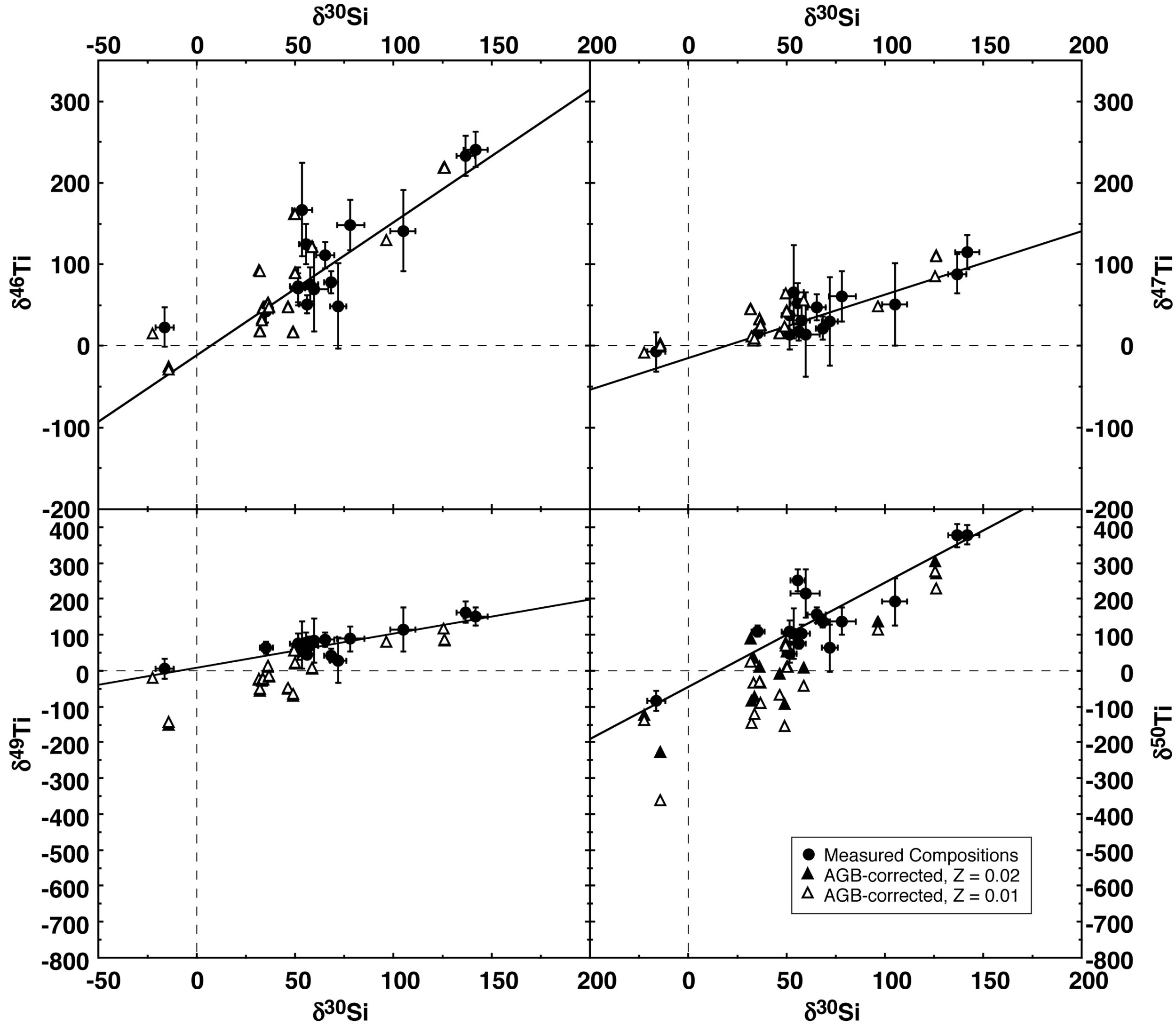

Fig 8. The measured delta values for titanium, plotted against δ^{30}Si, are compared with AGB-corrected initial compositions for the parent stars calculated based on stellar models with the new Guber et al. (2003) cross sections for silicon and two different stellar metallicities (Z), solar (0.02) and half of solar (0.01) (see text). The isotopic shifts are larger for lower metallicity. For both metallicities, the grains move down on the δ^{49}Ti and δ^{50}Ti plots, moving the array of inferred initial compositions farther from the solar composition.

The *s*-process contribution to the silicon isotopes in grain 317, while larger than for other grains in this study, is not large compared to Y and Z grains. It is also important to note that correcting for the *s*-process contribution shifts the compositions of the parent stars farther from the solar composition in ^{49}Ti/^{48}Ti and ^{50}Ti/^{48}Ti. This observation led Amari et al. (2001a) to conclude that the Sun has a very different titanium isotopic composition than did the parent stars of the silicon carbide grains. However, it is implausible that the Sun, whose composition arose by mixing the ejecta of thousands of stars, should have a composition that differs substantially from the compositions of the parent stars of silicon carbide grains, which also arose through mixing of the ejecta of thousands of stars. The newer silicon cross sections do not move the inferred initial titanium compositions as far away from the solar composition as did the earlier cross sections. This analysis indicates that the new silicon cross sections from Guber et al. (2003), which should be more accurate because of the improved experimental techniques, are in fact superior to the early ones. The same conclusion was reached by Zinner et al. (2006).

Let us next consider the potential role of metallicity. Figure 8 compares the measured compositions of the grains with compositions calculated from models assuming solar metallicity (0.02) and a metallicity of half of solar (0.01) (Lugaro et al. 1999; Amari et al. 2001a). The models used a standard ^{13}C pocket and Reimers mass-loss parameter η = 0.3. These models were coupled to models using the new silicon cross sections (Zinner et al. 2006) as described above. The inferred shifts from the initial composition due to *s*-process are larger for all of the isotopes in the low-metallicity model. This is due both to a higher temperature in the helium shell, which enhances the ^{22}Ne neutron source, and to the lower abundance of seed nuclei to interact with the neutrons. Calculations for lower metallicity (0.006) show even larger shifts (Amari et al. 2001a), and we would expect higher metallicity to show smaller shifts. However, note differences in inferred initial compositions due to changing metallicity are smaller than the differences due to changes in other parameters.

What criteria can be used to evaluate the plausible range of metallicity? The compositions calculated for metallicities of solar and half solar are, for the most part, not so extreme as to be a priori implausible. However, the calculation for grain 317 again implies that about half of the ^{50}Ti in the grain was produced in the parent star for the low-metallicity case. As already mentioned, the array of initial compositions should not pass too far from the solar composition, so solar or higher-than-solar metallicities would seem to be preferred. On this basis, we conclude that the parent stars for the majority of mainstream grains were most likely of at least solar metallicity, and Fig. 8 suggests that the metallicities higher than solar are not excluded. Plots versus δ^{29}Si give a similar picture.

We next consider stellar mass and mass-loss rate. The published models use different mass-loss prescriptions for different stellar masses, so these two parameters are coupled in this analysis, as they are in nature. Here we compare calculations of initial composition based on the standard model for a 1.5 $M_\odot$ star of solar metallicity calculated with a standard ^{13}C pocket and Reimers mass-loss parameter $\eta = 0.3$ (Lugaro et al. 1999; Zinner et al. 2006) with calculations based on a model for a 3.0 $M_\odot$ star of solar metallicity, a standard ^{13}C pocket and Reimers mass-loss parameter $\eta = 1.5$ (Lugaro et al. 1999; Zinner et al. 2006). We also include calculations based on a 5 $M_\odot$ model with solar metallicity, a standard ^{13}C pocket, and mass-loss parameter $\eta = 10$ (Amari et al. 2001a; Zinner et al. 2006). The 1.5 $M_\odot$ model is the same one shown for solar metallicity in Fig. 8. As before, we adjusted the delta silicon results for the literature models for new neutron capture cross sections based on results of Zinner et al. (2006).

The results of these calculations are shown in Fig. 9. AGB corrections based on the 1.5 $M_\odot$ model move most of the data to below the original regression lines for δ^{46}Ti, δ^{49}Ti, and δ^{50}Ti. Corrections based on the 5 $M_\odot$ model move the data in the opposite direction. The corrections based on the 3.0 $M_\odot$ model move the grain compositions almost parallel to the regression line, perhaps slightly upward for δ^{50}Ti. Although the results for the 5 $M_\odot$ model seem to move the arrays for δ^{46}Ti and δ^{50}Ti closer to the solar composition, there are good reasons to discount 5 $M_\odot$ stars. A 5 $M_\odot$ model could not match the measured compositions of Sr, Zr, Mo, and Ba in silicon carbide grains (Lugaro et al. 2003; Davis and Gallino 2006). In addition, stars of >4.5 $M_\odot$ may not become carbon stars because hot bottom burning at the base of the convective envelope during the AGB burns the carbon to ^{14}N (Boothroyd et al. 1993, 1995). Figure 9 thus suggests that the parent stars for the silicon carbide grains were on average 2–3 $M_\odot$ stars. These stellar masses are slightly higher than those inferred by previous workers (Nicolussi et al. 1997; Lugaro et al. 2003; Davis and Gallino 2006).

Finally, we consider the size of the ^{13}C pocket. As discussed above, the ^{13}C pocket does not yet arise in a self-consistent manner in the models and must be introduced in a parameterized way. The size of the ^{13}C pocket should affect ^{49}Ti and ^{50}Ti more strongly than the silicon isotopes, so the titanium data from silicon carbide should provide constraints on the size of the pocket. Figure 10 shows AGB-corrected compositions based on models using ^{13}C pockets three times smaller than the standard model and two times larger than the standard model (Lugaro et al. 1999). The models are for 1.5 $M_\odot$ stars and assume solar metallicity and a Reimers mass-loss parameter $\eta = 0.3$. The equivalent model using the standard ^{13}C pocket is the 1.5 $M_\odot$, solar metallicity model shown in Figs. 8 and 9. Figure 10 shows that a model with a twice-standard ^{13}C pocket shifts the compositions quite far from the original regression lines, indicating that the model calculates too much *s*-processing of titanium. As we have seen before, the model with the standard ^{13}C pocket also shifts the δ^{49}Ti and δ^{50}Ti values below the original regression lines, i.e., farther from the solar composition. In contrast, the model with a ^{13}C pocket one-third of the standard size shifts the original compositions essentially parallel to the regression lines. There is even a hint that the δ^{46}Ti values and δ^{50}Ti go up slightly, pulling the regression lines closer to the solar composition, while the δ^{49}Ti values go down, again pulling the regression line close to the solar composition. Thus, models of AGB stars with ^{13}C pockets between 1 and 0.3 times standard appear to provide reasonable matches to the data. These values are somewhat lower than previous studies have indicated (e.g., Barzyk et al. 2006; Davis and Gallino 2006).

Our analysis of the 16 >4 μm Orgueil silicon carbide grains as a group indicates that the parent stars of these grains were, on average, stars of 2–3 $M_\odot$ and solar or slightly higher than solar metallicity. Our analysis also indicates that stellar models should use the new cross sections for silicon isotopes from Guber et al. (2003) and that the ^{13}C pocket should be smaller than the "standard" value previously defined by Gallino et al. (1998).

Evaluating Data for Individual Orgueil Silicon Carbide Grains

We can test the validity of our conclusions by looking in detail at the compositions of individual Orgueil silicon carbide grains. Figure 11 shows the measured compositions

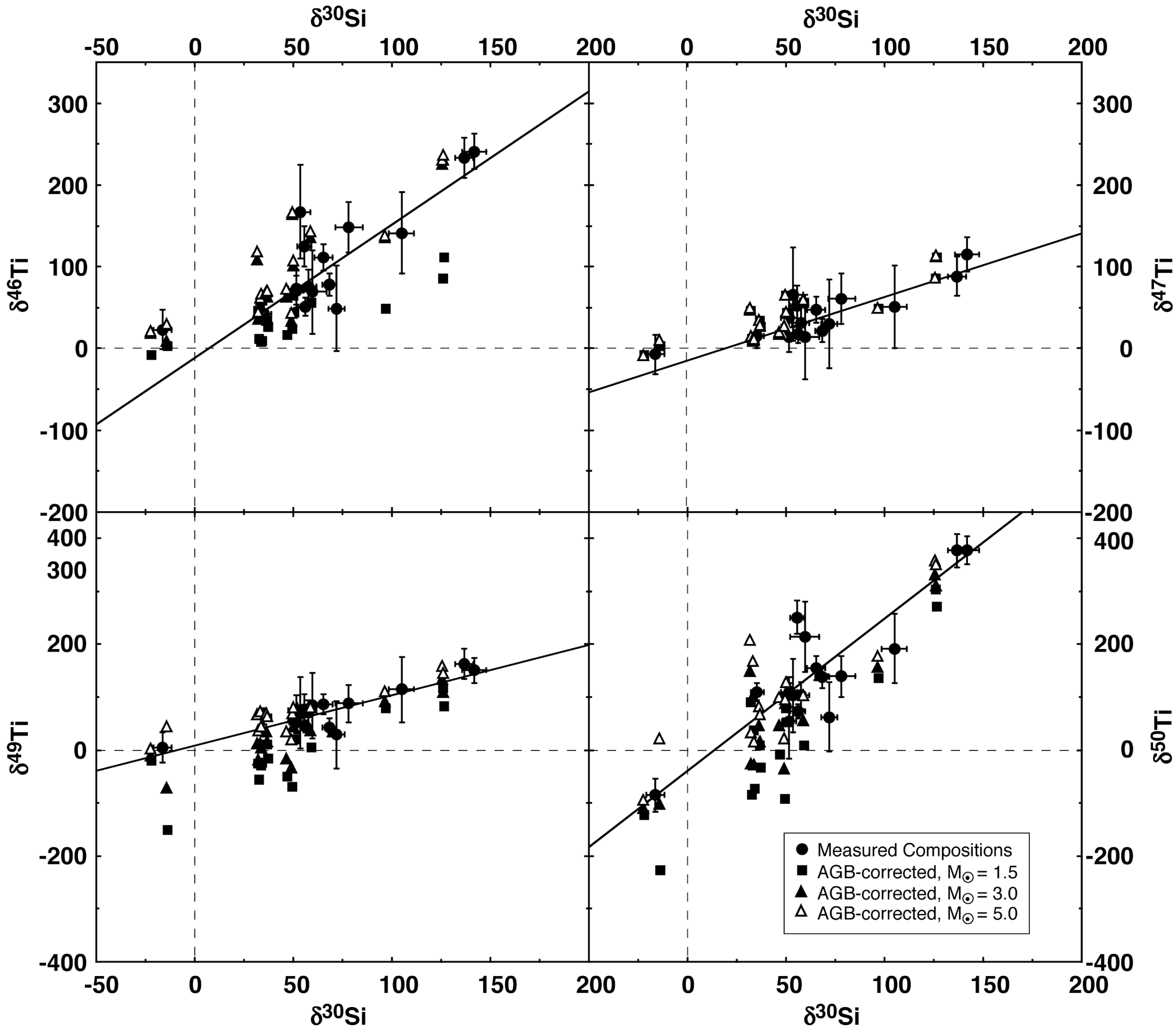

Fig. 9. The measured delta values for titanium, plotted against δ^{30}Si, are compared with AGB-corrected initial compositions for the parent stars calculated based on stellar models with the new Guber et al. (2003) cross sections for silicon and three different stellar masses (see text). The isotopic shifts for the 1.5 $M_\odot$ calculation are generally downward for ^{46}Ti, ^{49}Ti, and ^{50}Ti, but for the 5 $M_\odot$ calculation, the shifts are in the opposite direction. For the 3 $M_\odot$ model, the shifts are generally parallel with the arrays for all titanium isotopes.

of six Orgueil silicon carbide grains along with AGB-corrected compositions based on several of the models discussed above. The grains were chosen to cover the entire range of silicon compositions, and they are identified in Figs. 4, 5, and 6.

We will define "reasonable" AGB-corrected compositions to have the general characteristics expected from galactic chemical evolution. General considerations indicate that secondary isotopes, such as ^{29,30}Si and ^{46,47,49,50}Ti should increase with time in the galaxy (e.g., Clayton 1988). Timmes et al. (1995) calculated chemical and isotopic evolution trends for the elements hydrogen through zinc using the output of 60 supernova models from Woosley and Weaver (1995). Their calculation is able to produce the solar system abundances of most isotopes within a factor of two. In spite of the general success of this calculation, they are unable to match the isotopic compositions of the elements in detail. The titanium isotopes, except for ^{46}Ti, are under-produced by factors of 2–5 in this calculation, suggesting that stars other than the 11–40 $M_\odot$ stars considered in their calculation contributed to the solar composition. Although the Timmes et al. (1995) model has its shortcomings, it is the best model available with which to compare the compositions of the grains. In Fig. 12, we show $\delta^{46,47,49,50}$Ti values calculated from the output of the Timmes et al. (1995) model. Using the last part of the evolutionary trend, we calculated delta values for a 25% higher metallicity and 40% lower metallicity relative to an arbitrary composition from the Timmes et al. calculation

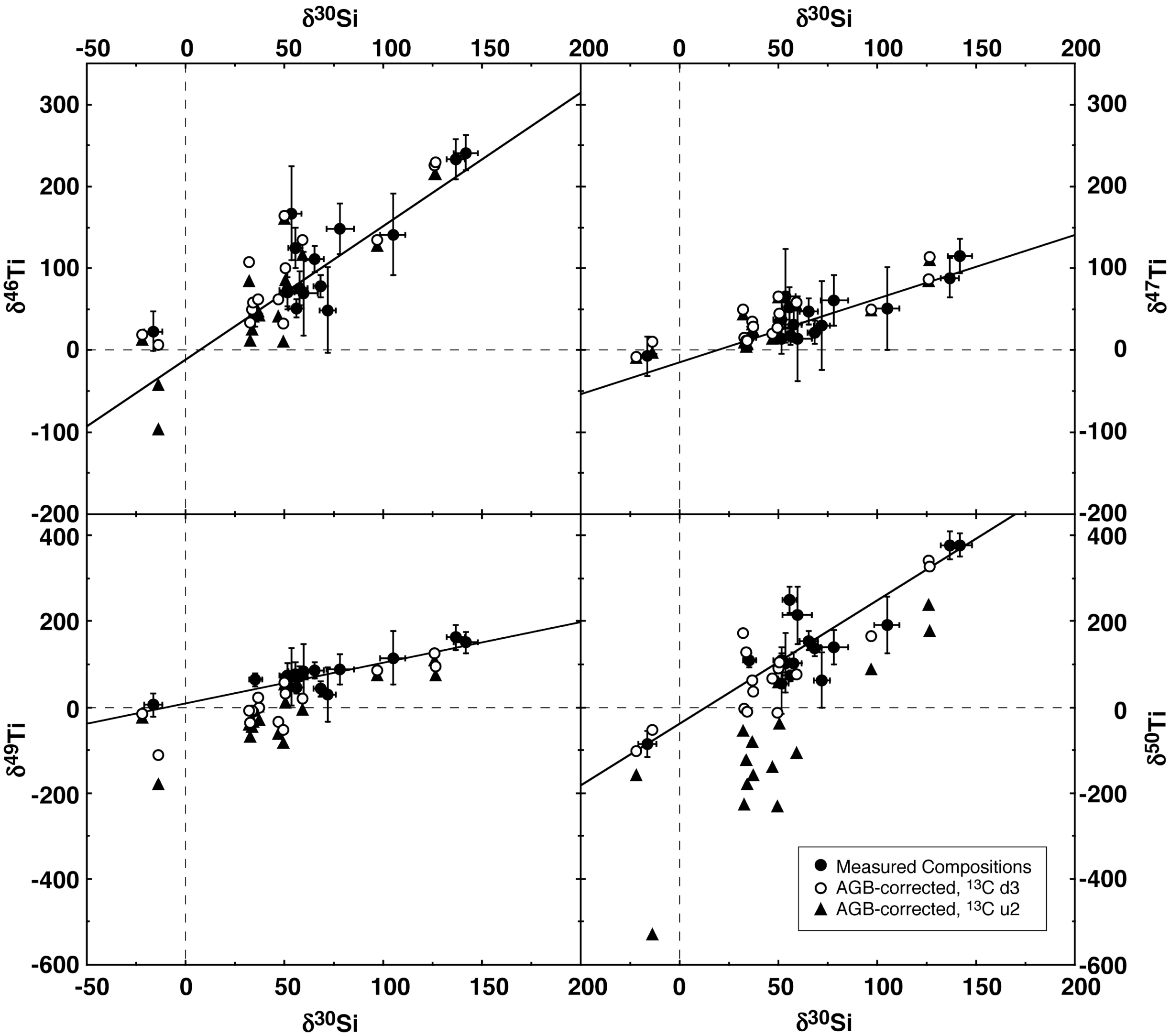

Fig. 10. The measured delta values for titanium, plotted against $\delta^{30}Si$, are compared with AGB-corrected initial compositions for the parent stars calculated based on stellar models with the new Guber et al. (2003) cross sections for silicon and two different parameterizations of the ^{13}C pocket, higher than standard by a factor of two (u2) and lower than standard by a factor of three (d3) (see text). The isotopic shifts for the model with twice-standard ^{13}C pocket are quite large, especially for ^{50}Ti, moving the inferred initial compositions of the parent stars far from the solar composition. In some cases the calculated compositions are implausible. In contrast, the isotopic compositions for the lower-than standard ^{13}C pocket shift approximately parallel to the arrays, and the small systematic deviations appear to push the arrays closer to the solar value.

for a time near when the Sun formed. These compositions show the trends of the evolution, not the absolute titanium abundances relative to the solar composition. Based on Fig. 12, we conclude that reasonable grain composition should show correlated excesses or deficits of the minor isotopes. Corrections for AGB contribution will affect $\delta^{49}Ti$ and $\delta^{50}Ti$ more than other isotopes, but the corrections should not produce an overall pattern with a character drastically different from expectations based on Fig. 12. The predicted patterns for the titanium isotopes match the measured patterns for the grains rather well, suggesting that the titanium in the grains is not dominated by the *s*-process contribution.

Grains 301 and 317 have slight $\delta^{29}Si$ deficits relative to the solar ratio (Fig. 6), and their parent stars may have had the lowest metallicities. Their titanium compositions are shown in Fig. 2 and at the top of Fig. 11. Grain 317 lies relatively far from the AGB-corrected array (Fig. 6) and thus has a significant AGB component in its silicon. It has $^{12}C/^{13}C = 65$, $^{15}N/^{14}N = 0.00018$, and inferred $^{26}Al/^{27}Al = 0.0006$. All of these features are consistent with a parent AGB star with active cool bottom processing (Wasserburg et al. 1995; Nollett et al. 2003), implying that the grain probably formed well into the carbon-star phase. Grain 301 lies very close to the AGB-corrected array (Fig. 6) and thus apparently has little

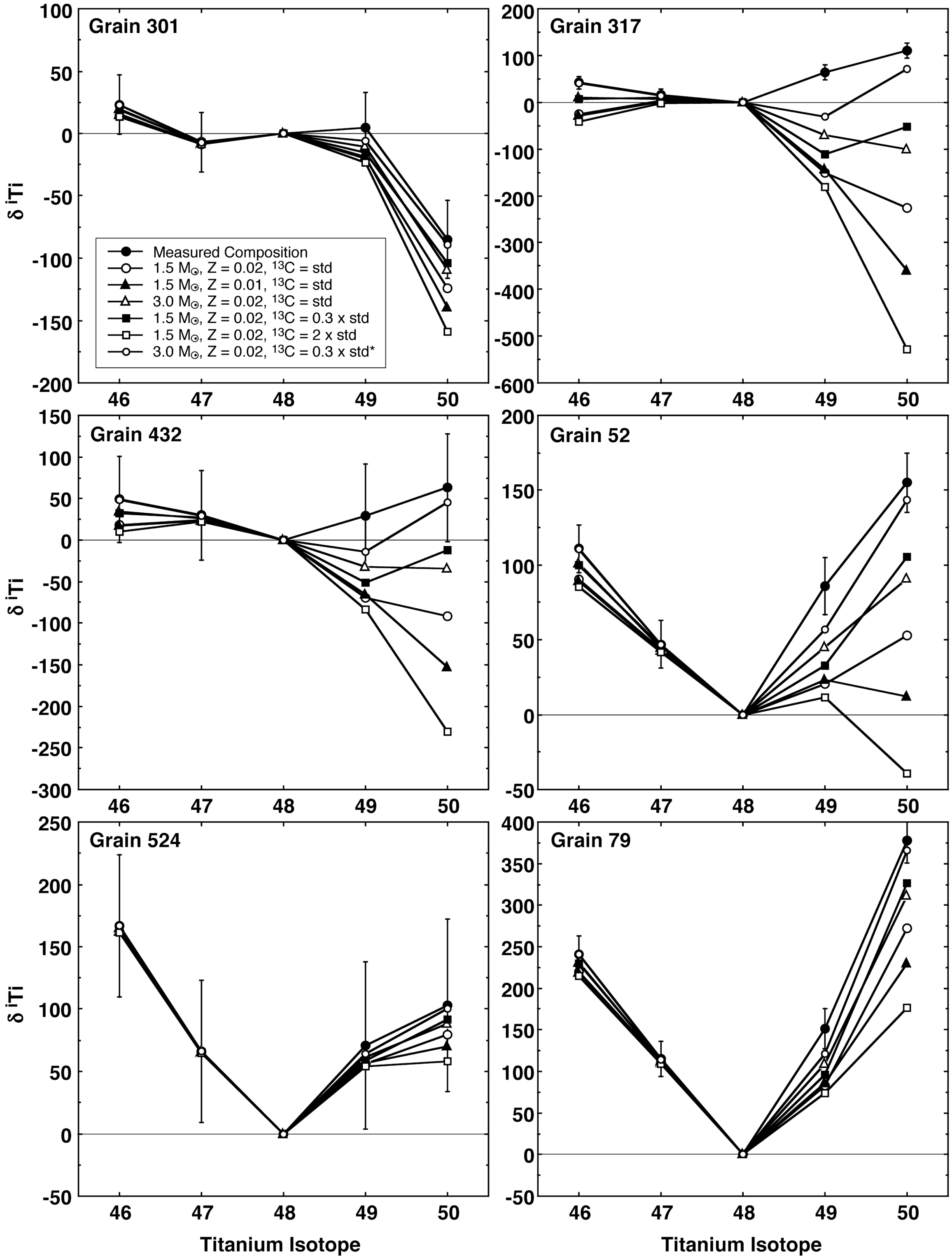

Fig. 11. Titanium compositions, plotted as delta values, for six Orgueil silicon carbide grains. For each grain, the measured composition is compared to compositions calculated by removing a supposed AGB component to derive the initial compositions of the parent stars. The plotted compositions are also plotted on Figs. 7–10. Note that the various models result in very different inferred initial compositions for the parent stars, particularly for grains with large *s*-process contributions to the silicon isotopes (Grains 317, 432, and 52; cf. Fig. 6). Models that produce the largest shifts for these three grains can probably be excluded because such shifts are implausible.
*Model derived by combining the results for a 3.0 $M_{\odot}$ solar metallicity model with a 0.3 times standard ^{13}C pocket (see text).

AGB silicon. It has $^{12}C/^{13}C$ = 5.3 and a $^{15}N/^{14}N$ ratio just below solar (0.00252) and was interpreted by Huss et al. (1997) to have come from a star that experienced a little cool bottom processing and to have formed just after the star became carbon-rich. However, this interpretation may work only if the parent star had a very unusual initial composition (cf. Nollet et al. 2003).

Because of the large *s*-process contribution to its silicon and, therefore, its titanium, the titanium isotopes of grain 317 provide relatively strong constraints on the parameters of the stellar models. The three models that generate the largest shifts in δ^{50}Ti for grain 317 imply that between 35% and 60% of the ^{50}Ti was produced in the parent star. These models also turn excesses in δ^{49}Ti and δ^{50}Ti into large deficits, while leaving δ^{46}Ti and δ^{47}Ti near solar. Because Grain 301 apparently has only a very small *s*-process contribution, its titanium isotopes are not strongly affected by any of the models. This grain can therefore provide an example of a plausible initial composition for a grain with $\delta^{29,30}$Si slightly lower than solar. The three models that produce the largest shifts in δ^{50}Ti all produce inferred initial compositions of the parent star with δ^{50}Ti below the composition of grain 301 or its parent star. These models would thus seem to be ruled out, so on this basis we rule out the model used by Lugaro et al. (1999) and Amari et al. (2001a), which is for a 1.5 $M_{\odot}$ star with solar metallicity and a standard ^{13}C pocket, and the 1.5 $M_{\odot}$ models with low metallicity or a ^{13}C pocket twice standard.

The 3.0 $M_{\odot}$ star with a standard ^{13}C pocket generates small depletions in ^{49}Ti and ^{50}Ti relative to solar for the parent star of grain 317, and so would be consistent with its silicon isotopes, implying a metallicity for the parent star slightly lower than solar. This model and the 1.5 $M_{\odot}$ model with a ^{13}C pocket 0.3 times standard give shifts of similar magnitude in δ^{49}Ti and δ^{50}Ti, although the patterns differ. We did not have a model for a 3 $M_{\odot}$ star with ^{13}C pocket 0.3 times standard. However, we simulate the output of such a model by calculating the difference in the compositions from the standard model and the standard model with ^{13}C pocket 0.3 times standard and then adding that difference to the 3.0 $M_{\odot}$ model output. The resulting pattern, shown in the small open circles, has excesses in $\delta^{46,47,50}$Ti and a slight deficit in δ^{49}Ti. These three models are plausible for both grains 317 and 301. For grain 317, models and the other isotopic data for grain 317 imply that the parent star was 1.5–3 $M_{\odot}$ well into its carbon-star phase with a metallicity similar to or slightly lower than solar and a ^{13}C pocket smaller than the standard pocket. Though fewer constraints are provided for the parent star of grain 301, a metallicity slightly lower than solar, a mass of 2–3 $M_{\odot}$, and a smaller-than-standard ^{13}C pocket are indicated.

Grains 432, 52, and 524 fall in the middle of the measured range of silicon isotope compositions (Fig. 6). These grains show a significant range in the size of the AGB contribution, as estimated from silicon isotopes (Fig. 6).

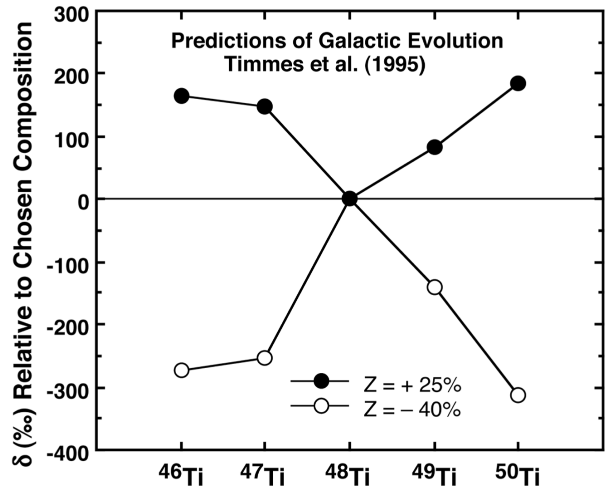

Fig. 12. Predicted trends for the titanium isotopes as a function of metallicity based on the galactic evolution model of Timmes et al. (1995). The patterns were generated by choosing an arbitrary composition close in the time coordinates of the model to when the solar system formed as a base composition and calculating delta values relative to this composition for metallicities 25% higher and 40% lower then the chosen composition. The plot thus shows the trends expected for titanium isotopes as a function of metallicity based on the model.

Grain 432 has the largest AGB correction among the three grains, and thus is the most sensitive to model parameters. It has a $^{12}C/^{13}C$ = 22; $^{15}N/^{14}N$ = 0.0014, and an inferred $^{26}Al/^{27}Al$ = 0.008, ten times higher than in the other grains. Huss et al. (1997) tentatively interpreted this grain to come from a star of <2.3 $M_{\odot}$, although all features are not explained by this interpretation. Grain 52 has the next largest AGB contribution as inferred from silicon isotopes. It has $^{12}C/^{13}C$ = 51, $^{15}N/^{14}N$ = 0.0008, and $^{26}Al/^{27}Al$ = 0.0009, compositions consistent with a typical carbon star (Huss et al. 1997). Grain 524 lies almost on the AGB-corrected correlation line and thus has the smallest correction of the three grains. This grain has $^{12}C/^{13}C$ = 49.5, $^{15}N/^{14}N$ = 0.00045, and inferred $^{26}Al/^{27}Al$ = 0.0008, all consistent with a typical carbon star relatively early in the AGB phase (Huss et al. 1997).

The measured compositions of all three grains show excesses in all of the minor titanium isotopes (Fig. 11). This is consistent with their excesses of silicon isotopes (Fig. 6). One would expect, therefore, that the AGB correction should not produce radically different initial compositions for the three grains, although note that grain 432 has smaller $\delta^{46,47,49,50}$Ti excesses than do the other two grains. Grain 524 provides a reasonable idea of the titanium compositions for the parent stars. Based on this criterion, we can eliminate several models. The most extreme model composition for the parent star of grain 432 has larger deficits of $\delta^{49,50}$Ti than the measured composition or all of the models for grain 301. The same model produced negative δ^{50}Ti for grain 52. This model is thus unreasonable. In fact, the extreme negative $\delta^{49,50}$Ti calculated for the parent star of grain 432 probably rule out the three most extreme models, the model used by Lugaro et al. (1999) and Amari et al. (2001a), which is for a 1.5 $M_\odot$ star with solar metallicity and a standard ^{13}C pocket, and the 1.5 $M_\odot$ models with low metallicity or a ^{13}C pocket twice standard. The other compositions are all plausible, although note that two of the models result in negative $\delta^{49,50}Ti$ for grain 432. This cannot be entirely excluded because of the lower excess of minor titanium isotopes in the measured composition, perhaps implying a lower metallicity.

The acceptable models for the parent stars of grains 432, 52, and 524 include two 3-$M_\odot$ models, one with solar metallicity and standard ^{13}C pocket and one with solar metallicity and 0.3 times standard ^{13}C pocket, and one 1.5-$M_\odot$ model with solar metallicity and 0.3 times standard ^{13}C pocket. The common theme in these models is higher mass and smaller than standard ^{13}C pocket. Higher-than-solar metallicity is not excluded for grains 52 and 524, although it may be for grain 432.

Grain 79 has the largest excesses of $\delta^{29,30}Si$ relative to the solar composition and requires a moderate AGB correction to move it to the AGB-corrected correlation line. This grain has $^{12}C/^{13}C$ = 41, $^{15}N/^{14}N$ = 0.00028, and inferred $^{26}Al/^{27}Al$ = 0.0008, typical values for carbon stars (Huss et al. 1997). For this grain, excesses of minor titanium isotopes are so large that none of the corrected compositions have negative $\delta^{50}Ti$. Therefore, none of the models can be excluded because they produce unreasonable initial compositions. However, a low-metallicity parent star seems to be unlikely because of the large excesses of minor titanium isotopes and because there does seem to be a correlation between excesses in minor titanium isotopes and metallicity.

Our analysis of data for individual grains leads to the following conclusions: 1) Models with ^{13}C pockets larger than the standard model seem to be ruled out for nearly all of the grains and models with standard ^{13}C pockets also seem to result in too large of shifts in titanium isotopes for most of the grains. 2) Stars more massive than 1.5 $M_\odot$ seem to be indicated, although other criteria, such as modeling of heavy *s*-process elements, seem to limit the masses to ≤3 $M_\odot$. 3) We do not have clear-cut evidence on metallicity, but the grains seem to follow the general expectation from galactic chemical evolution. Note, however, that grains 432, 52, and 524, which have very similar silicon compositions, have different titanium compositions and may have come from stars of different metallicity. This inference, if it is confirmed, would support the idea that metallicity and isotopic compositions do not exactly track each other and that stochastic variations in contributions from nucleosynthetic sources (Lugaro et al. 1999) play a role in the compositions and metallicities of the parent stars.

Comparison of Our Results with Evidence from Other Sources

Our results based on the population of 16 silicon carbide grains are, in general, consistent with the results derived from individual grains. Both analyses indicate that parent stars were between 1.5 and 3 $M_\odot$, which is consistent with results of previous workers. Both analyses imply metallicities of solar to somewhat higher than solar (although parent stars of a handful of grains may have had slightly lower metallicities). And, models with ^{13}C pockets somewhat smaller than the standard pocket defined by Gallino et al. (1998) do the best job of matching the measurements.

It is useful to compare our conclusions based on silicon and titanium isotopes to those based on other data sets. An important constraint comes from modeling the compositions of strontium, zirconium, molybdenum, and barium measured in individual silicon carbide grains by resonance ionization mass spectrometry (RIMS) (Nicolussi et al. 1997, 1998a, 1998b; Savina et al. 2003; Barzyk et al. 2006). Strontium, zirconium, and barium are affected by branching in the *s*-process path (e.g., Lugaro et al. 2003). Models of 1.5, 2, 3, and 5 $M_\odot$, with a range of metallicities and ^{13}C pockets from 0.08 times standard to 2 times standard have been calculated (Lugaro et al. 2003; Davis and Gallino 2006). These models best reproduce the results from the silicon carbide grains with parent stars with masses of 1.5–3 $M_\odot$, with most grains coming from stars at the lower end of the range, solar metallicity, and ^{13}C pockets from 0.67 times standard to 1.3 times standard (Lugaro et al. 2003; Davis and Gallino 2006). These results are generally consistent with our analysis, except that they imply lower stellar masses and larger ^{13}C pockets than our results. In order to reconcile our conclusions with theirs, we must find a way to lower the shifts in ^{49}Ti and ^{50}Ti indicated by our modeling. One possibility is that the grains measured in our study and those measured for heavy elements by RIMS represent different subsets of the silicon carbide population. Grains forming from stars with small ^{13}C pockets might not generate enough *s*-process heavy elements for analysis by RIMS (Barzyk et al. 2006). However, a significant fraction of grains with low *s*-process-element contents would be required for this explanation to be correct. Alternatively, the neutron-capture cross sections for ^{49}Ti and ^{50}Ti used in the models that were the basis for our study may be too low. Slightly higher cross sections for ^{49}Ti and ^{50}Ti would produce smaller excesses in the models, removing the apparent requirement for higher mass, higher metallicity, and smaller ^{13}C pockets.

Galactic Chemical Evolution and the Metallicity in Silicon Carbide Parent Stars

Like earlier workers, we conclude that the arrays of silicon and titanium isotopic compositions found for silicon carbide grains primarily reflect the initial compositions of the parent stars with only a small overprint from nucleosynthesis in those stars. Most silicon carbide grains exhibit excesses of $^{29,30}Si$ and $^{46,47,49,50}Ti$ relative to solar silicon and titanium (Figs. 2–6). Aluminum oxide grains also tend to show correlated excesses or deficits of minor magnesium and titanium isotopes and inferred initial ^{18}O (e.g., Alexander and Nittler 1999). The general view is that minor isotopes of oxygen, magnesium, silicon, and titanium (“secondary” isotopes) increase with time relative to the “primary” isotopes (e.g., ^{16}O, ^{24}Mg, ^{28}Si, ^{48}Ti), which can be produced directly from hydrogen and helium by stellar nucleosynthesis (e.g., Clayton 1988; Timmes et al. 1995). The secondary isotopes ($^{29,30}Si$, $^{46,47,49,50}Ti$) can only be produced if sufficient amounts of primary isotopes were inherited by the star. Thus, $^{29,30}Si$ and $^{46,47,39,50}Ti$ should be increasing in abundance relative to ^{28}Si and ^{48}Ti with time in the galaxy. The corollary to this is that stars that lived and died prior to the formation of the Sun, might be expected to have lower relative abundances of these minor isotopes (if all formed in the same region of the galaxy), not higher, as observed.

There are two types of solutions to this dilemma. One can take the observations and their obvious implication at face value and try to understand how they arose, or one can try to find an explanation that does not require the silicon carbide parent stars to have higher metallicity than the Sun. A possible solution of the first type was suggested by Clayton (1997), who proposed that the parent stars of the silicon carbide grains formed closer to the galactic center, where metallicity and secondary isotope abundances are higher, than the Sun did and diffused outward into the solar neighborhood before they ejected silicon carbide into the interstellar medium. Alternatively, the Sun might have incorporated the ejecta of a supernova, which would have been enriched in primary isotopes relative to the original composition (e.g., Alexander and Nittler 1999 and references therein). Lugaro et al. (1999) proposed a solution of the second type. They recognized that galactic chemical evolution is stochastic in nature due to the episodic injections of newly synthesized material from dying stars and relatively slow galactic mixing. Therefore, isotopic compositions will be heterogeneous and will not precisely track metallicity. They constructed a simple Monte Carlo model in which contributions from various types of supernova were admixed in a statistical way with a given silicon composition. By adding different amounts of material from the different types of supernova to four distinct starting compositions, they were able to reproduce the spread in silicon isotopic composition of silicon carbide grains. They conclude that it is not necessary to suppose that the compositions of the parent stars of the silicon carbide grains represent galactic evolution in the classic sense; instead they could reflect local heterogeneities in the composition of the interstellar medium. While this is an interesting idea that is based on a real phenomenon, it is unlikely that the silicon and titanium arrays for silicon carbide grains reflect only local heterogeneities. Nittler (2005) has argued that because silicon and titanium isotope yields in supernova are decoupled, stochastic mixing models cannot explain the silicon-titanium correlations shown in Figs. 4 and 5. Galactic evolution has certainly occurred and unless the masses (and thus the lifetimes) of the silicon carbide parent stars were all identical, they must have formed over an extended period of time, allowing them to pick up the signature of galactic chemical evolution.

Therefore, we find no compelling reason to ignore the obvious interpretation that the silicon and titanium isotopic compositions of the parent stars of most mainstream silicon carbide grains had metallicities similar to or higher than that of the Sun. Our study of silicon and titanium isotopic compositions provides some support for higher-metallicity parent stars for many silicon carbide grains. Our data also provide some support for the idea that isotopic composition and metallicity do not vary in lock-step, although this seems to be a second-order effect superimposed on the general trend. Resolution of this question will require considerable additional modeling.

SUMMARY AND CONCLUSIONS

In this paper, we have reported titanium-isotope data for 23 >4 μm presolar silicon carbide grains from the Orgueil CI chondrite for which Huss et al. (1997) had previously collected isotopic data for silicon, carbon, nitrogen, and magnesium. We discussed the 16 grains with the best-determined compositions in the context of detailed models of nucleosynthesis in AGB stars. We agree with previous workers that the silicon and titanium isotope arrays exhibited by presolar silicon carbide grains reflect primarily the initial compositions of the parent stars overprinted by a relatively small component of *s*-process nucleosynthesis. Our analysis of several parameters in the stellar models, including stellar mass, metallicity, neutron-capture cross sections, the size of the ^{13}C pocket, and mass-loss rate lead to the following conclusions: 1) the parent stars of the silicon carbide grains were typically 2–3 $M_\odot$ stars of a range of metallicity from slightly less than solar to somewhat greater than solar; 2) the new neutron-capture cross sections for silicon from Guber et al. (2003) are superior to the older values; 3) models with ^{13}C pockets somewhat smaller than the “standard” pocket used by Gallino et al. (1997, 1998), Lugaro et al. (1999), and Amari et al. (2001a) produce the best matches to the titanium data from the silicon carbide grains; 4) the composition of the Sun lies on or very close to the array of initial compositions of the stars that produced the silicon carbide grains; and 5) the Sun does lie at the low-metallicity end of the silicon and titanium arrays defined by the parent stars of mainstream grains. Although these results are generally consistent with the inferences from previous studies, we infer slightly higher masses and slightly smaller ^{13}C pockets than did the authors modeling *s*-process heavy elements. The slight differences between our results and those of previous workers might be understood in terms of differences in the subsets of samples that were studied, but they might be brought into better agreement if it turns out that the neutron-capture cross sections for ^{49}Ti and ^{50}Ti are slightly higher than those current used in the models.

Acknowledgments–We thank Frank Timmes for access to the numerical output from the models for Timmes et al. (1995), Larry Nittler for providing a copy of his database of compositions for presolar silicon carbide grains, and Maria Lugaro for helpful discussions. The paper also benefited from detailed reviews by Roberto Gallino, Andrew Davis, and Larry Nittler. Supported by NASA grants NAG5-11543 and NNG05GG48G to G. R. H.

Editorial Handling—Dr. Larry Nittler

REFERENCES

Alexander C. M. O'D. and Nittler L. R. 1999. The galactic evolution of Si, Ti, and O isotopic ratios. *The Astrophysical Journal* 519: 222–235.

Amari S. Nittler L. R., Zinner E., Gallino R., Lugaro M., and Lewis R. S. 2001a. Presolar SiC grains of type Y: Origin from low-metallicity asymptotic giant branch stars. *The Astrophysical Journal* 546:248–266.

Amari S., Nittler L. R., Zinner E., Lodders K., and Lewis R. S. 2001b. Presolar grains of type A and B: Their isotopic compositions and stellar origins. *The Astrophysical Journal* 559:463–483.

Barzyk J. G., Savina M. R., Davis A. M., Gallino R., Pellin M. J., Lewis R. S., Amari S., and Clayton R. N. 2006. Multi-element isotopic analysis of single presolar SiC grains. *New Astronomy Reviews* 50:587–590.

Barnes I. L., Moore L. J., Machlan L. A., Murphy T. J., and Shields W. R. 1975. Absolute isotopic abundance ratios and the atomic weight of a reference sample of silicon. *Journal of Research of the National Bureau of Standards* 79a:727–735.

Bao Z. Y., Beer H., Käppler F., Voss F., Wisshak K., and Rauscher T. 2000. Neutron cross sections for nucleosynthesis studies. *Atomic Data and Nuclear Data Tables* 76:70–154.

Bernatowicz T. J., Cowsik R., Gibbons P. C., Lodders K., Fegley B., Jr., Amari S., and Lewis R. S. 1996. Constraints of stellar grain formation from presolar graphite in the Murchison meteorite. *The Astrophysical Journal* 472:760–782.

Boldeman J. W., Allen B. J., de L. Musgrove A. R., and Macklin R. L. 1975. The neutron capture cross section of natural silicon. *Nuclear Physics A* 252:62–76.

Boothroyd A. I., Sackmann I.-J., and Ahern S. C. 1993. Prevention of high-luminosity carbon stars by hot bottom burning. *The Astrophysical Journal* 416:762–768.

Boothroyd A. I., Sackmann I.-J., and Wasserburg G. J. 1995. Hot bottom burning in asymptotic giant branch stars and its effect of oxygen isotopic abundances. *The Astrophysical Journal* 442: L21–L24.

Clayton D. D. 1988. Isotopic anomalies: Chemical memory of galactic chemical evolution. *The Astrophysical Journal* 334: 191–195.

Clayton D. D. 1997. Placing the Sun and mainstream SiC particles in galactic chemodynamic evolution. *The Astrophysical Journal* 484:L67–L70.

Davis A. M. and Gallino R. 2006. Heavy elements in presolar grains: constraints on conditions in asymptotic giant branch stars. Proceedings, Science-Nucleii in the Cosmos-IX. http://pos.sissa.it//archive/conferences/028/018/NIC-IX_018.pdf.

Dearborn D. S. P. 1992. Diagnostics of stellar evolution: The oxygen isotopes. *Physics Reports* 210:367–382.

Forestini M., Paulus G., and Arnould M. 1991. On the production of ^{26}Al in AGB stars. *Astronomy and Astrophysics* 252:597–604.

Gallino R., Raiteri C. M., Busso M., and Matteucci F. 1994. The puzzle of silicon, titanium, and magnesium anomalies in meteoritic silicon carbide grains. *The Astrophysical Journal* 430: 858–869.

Gallino R., Busso M., and Lugaro M. 1997. Neutron capture nucleosynthesis in AGB stars. In *Astrophysical implications of the laboratory study of presolar materials*, edited by Bernatowicz T. K. and Zinner E. AIP Conference Proceedings. pp. 115–153.

Gallino R., Arlandini C., Busso M., Lugaro M., Travaglio C., Straniero O., Chieffi A., and Limongi M. 1998. Evolution and nucleosynthesis in low-mass asymptotic giant branch stars. II. Neutron capture and the *s*-process. *The Astrophysical Journal* 497:388–403.

Guber K. H., Koehler P. E., Derrien H., Valentine T. E., Leal L. C., Sayer R. O., and Rauscher T. 2003. Neutron capture reaction rates for silicon and their impact on the origin of presolar mainstream SiC grains. *Physical Review C* 67:062802(R).

Gyngard F., Amari S., Jadhav M., Marhas K., Zinner E., and Lewis R. S. 2006. Titanium isotopic ratios in KJG presolar SiC grains from Murchison (abstract). *Meteoritics & Planetary Science* 41: A71.

Hoppe P. and Besmehn A. 2002. Evidence for extinct vanadium-49 in presolar silicon carbide grains from supernovae. *The Astrophysical Journal* 576:L69–L72.

Hoppe P., Amari S., Zinner E., Ireland T., and Lewis R. S. 1994. Carbon, nitrogen, magnesium, silicon, and titanium isotopic compositions of single interstellar silicon carbide grains from the Murchison carbonaceous chondrite. *The Astrophysical Journal* 430:870–890.

Huss G. R. and Lewis R. S. 1995. Presolar diamond, SiC, and graphite in primitive chondrites: Abundances as a function of meteorite class and petrologic type. *Geochimica et Cosmochimica Acta* 59: 115–160.

Huss G. R., Hutcheon I. D., and Wasserburg G. J. 1997. Isotopic systematics of presolar silicon carbide in the Orgueil (CI) chondrite: Implications for solar system formation and stellar nucleosynthesis. *Geochimica et Cosmochimica Acta* 61:5117–5148.

Iben I., Jr. and Renzini A. 1983. Asymptotic giant branch evolution and beyond. *Annual Reviews of Astronomy and Astrophysics* 21: 271–342.

Lugaro M., Zinner E., Gallino R., and Amari S. 1999. Si isotope ratios in mainstream presolar SiC grains revisited. *The Astrophysical Journal* 527:369–394.

Lugaro M., Davis A. M., Gallino R., Pellin M. J., Straniero O., and Käppeler F. 2003. Isotopic compositions of strontium, zirconium, molybdenum, and barium in single presolar SiC grains and asymptotic giant branch stars. *The Astrophysical Journal* 593:486–508.

Nicolussi G. K., Davis A. M., Pellin M. J., Lewis R. S., Clayton R. N., and Amari S. 1997. *s*-process zirconium in presolar silicon carbide grains. *Science* 277:1281–1283.

Nicolussi G. D., Pellin M. J., Lewis R. S., Davis A. M., Amari S., and Clayton R. N. 1998a. Molybdenum isotopic compositions of individual presolar silicon carbide grains from the Murchison meteorite. *Geochimica et Cosmochimica Acta* 62: 1093–1104.

Nicolussi G. D., Pellin M. J., Lewis R. S., Davis A. M., Amari S., and Clayton R. N. 1998b. Strontium isotopic composition in individual circumstellar silicon carbide grains: A record of *s*-process nucleosynthesis. *Physical Review Letters* 81:3583–3586.

Niederer F. R., Papanastassiou D. A., and Wasserburg G. J. 1985. Absolute isotopic abundances of Ti in meteorites. *Geochimica et Cosmochimica Acta* 49:835–851.

Nittler L. R. 2005. Constraints on heterogeneous galactic chemical evolution from meteoritic stardust. *The Astrophysical Journal* 618:281–296.

Nittler L. R. and Hoppe P. 2005. Are presolar silicon carbide grains from novae actually from supernovae? *The Astrophysical Journal* 631:L89–L92.

Nittler L. R., Amari S., Zinner E., Woosley S. E., and Lewis R. S. 1996. Extinct ^{44}Ti in presolar graphite and SiC: Proof of a supernova origin. *The Astrophysical Journal* 462:L31–L34.

Nollett K. N., Busso M., and Wasserburg G. J. 2003. Cool bottom processing on the thermally pulsing asymptotic giant branch and the isotopic composition of circumstellar dust grains. *The Astrophysical Journal* 582:1036–1058.

Reimers D. 1975. Circumstellar envelopes and mass loss of red giant stars. In *Problems in stellar atmospheres and envelopes*, edited by Baschek B., Kegel W. H., and Traving G. New York: Springer-Verlag. pp. 229–256.

Savina M. R., Davis A. M., Tripa C. E., Pellin M. J., Clayton R. N., Lewis R. S., Amari S., Gallino R., and Lugaro M. 2003. Barium isotopes in individual presolar silicon carbide grains from the Murchison meteorite. *Geochimica et Cosmochimica Acta* 67:3201–3214.

Smith J. B. and Huss G. R. 2002. Titanium isotopes in presolar SiC grains from Orgueil (abstract). *Meteoritics & Planetary Science* 37:A134.

Stone J., Hutcheon I. D., Epstein S., and Wasserburg G. J. 1991b. Silicon, carbon, and nitrogen isotopic studies of silicon carbide in carbonaceous and enstatite chondrites. In *Stable isotope geochemistry: A tribute to Samuel Epstein*, edited by Taylor H. P., Jr., O'Neil J. R., and Kaplan I. R. Geochemical Society Special Publication #3. pp. 487–504.

Straniero O., Chieffi A., Limongi M., Busso M., Gallino R., and Arlandini C. 1997. Evolution and nucleosynthesis in low-mass asymptotic giant branch stars. I. Formation of Population I carbon stars. *The Astrophysical Journal* 478:332–339.

Straniero O., Gallino R., and Cristallo S. 2006. *s*-process in low-mass asymptotic giant branch stars. *Nuclear Physics A* 777:311–339.

Timmes F. S., Woosley S. E., and Weaver T. A. 1995. Galactic chemical evolution: Hydrogen through zinc. *The Astrophysical Journal* 98:617–658.

Wasserburg G. J., Boothroyd A. I., and Sackmann I.-J. 1995. Deep circulation in red giant stars: A solution to the carbon and oxygen isotope puzzles. *The Astrophysical Journal* 263:891–901.

Wilson R. G. and Novak S. W. 1991. Systematics of secondary ion mass spectrometry relative sensitivity factors versus electron affinity and ionization potential for a variety of matrices determined from implanted standards of more than 70 elements. *Journal of Applied Physics* 69:466–474.

Woosley S. E. and Weaver T. A. 1995. The evolution and explosion of massive stars. II. Explosive hydrodynamics and nucleosynthesis. *The Astrophysical Journal* 101:181–235.

Zinner E., Nittler L. R., Gallino R., Karakas A. I., Lugaro M., Staniero O., and Lattanzio J. C. 2006. Silicon and carbon isotopic ratios in AGB stars: SiC grain data, models, and the galactic evolution of the Si isotopes. *The Astrophysical Journal* 650:350–373.